Chapter 7

OCEANIC GENERAL CIRCULATION MODELS

1 Introduction

The ultimate expression of our understanding of the dynamical processes that control circulation is an Oceanic General Circulation Model (OGCM), since no theory nor simpler model can represent the full combination of geographically complex forcing patterns and domain shapes, advection, and rectification. Here is a description of how to formulate such a model. It is adapted from the review paper by McWilliams (1998). A more recent and comprehensive review of OGCM practices in global circulation and climate modeling is Griffies (2004).

The practice of oceanic numerical modeling is growing rapidly. Several reasons for this are the following:

- a widespread realization that model solutions can, either now or at least in the near future, be skillful in mimicking observed oceanic features;
- an understanding of the limitations of the more traditional scientific methodologies of making measurements in the ocean and developing analytic theories for highly nonlinear dynamical systems;
- an appreciation of the importance of the oceans in the socially compelling problems of anthropogenic changes in climate and the environment; and
- an exploitation of the steady increase in computing power that makes meaningfully comprehensive oceanic calculations ever more feasible.

The oceanic general circulation is defined as the currents on horizontal space and time scales larger than the mesoscale (of order 100 km and 3 months), and it includes the associated pressure, density, temperature, and salinity fields, plus all other elements involved in establishing the dynamical balances for these fields. The latter are the forcing fields, domain geometry, and large-scale transport contributions from currents on meso- and micro-scales. In some contexts the general circulation also includes biogeochemical and anthropogenic processes associated with other material property fields such as nitrate, carbon dioxide, or freon. The term tracers denotes the scalar variables moving with fluid parcels, including temperature T and salinity S, which influence currents through the density ρ in the gravitational force.

This section gives an overview of the formulation of OGCMs and some illustrations of typical solutions. OGCMs are defined as numerical models that include all of the major influences on

the general circulation, constrained by limitations both in our knowledge about how to formulate the model and in the available computing power. Of course, this is a somewhat loose definition, but I take it to imply that OGCMs necessarily have wind, heat, and water forcing, geographically correct domain geometry, and the equation of state for seawater — all with their inescapable approximations; models simpler than this should be called idealized process models.

Why are OGCMs useful? It is obvious that they would be so for studying ocean currents, but they have many other important applications as well:

- dynamical coupling with the atmosphere, sea ice, and land run-off that in reality jointly determine the oceanic boundary fluxes (*e.g.,* El Niño);
- transport of biogeochemical materials;
- interpretation of the paleoclimate record;
- climate prediction for both natural variability and anthropogenic changes (especially warming, acidification, and harvesting);
- assimilation of sparse measurements to provide dynamically consistent interpolations and syntheses;
- pollution dispersal; and
- fisheries and other ecosystem management.

The scientific practices of using OGCMs include continual model development to improve their accuracy; tests against observations to assess model accuracy; and solution analyses to explain how different physical influences combine and compete to produce the general circulation. A particularly instructive way to use an OGCM, once it has captured some particular behavior of interest, is to systematically reduce its component processes to distill the essential cause. Particularly interesting uses of OGCMs are to explore hypothetical realities, such as the ocean circulation of ancient earth epochs, the consequences of deliberate biological fertilization of the oceans, or future climates under alternative planetary management strategies.

2 Model Formulation

2.1 Dynamics

Broadly summarized, the historical development and utilization path for OGCMs is firstly to model only the largest scales of motion with an excessively coarse numerical grid and a concomitant excessively linear and diffusive dynamics, where the " eddy diffusion" represents the effects of (*i.e.,*

parameterizes) the unresolved (*i.e.,* sub-grid-scale, SGS) currents. Subsequently, more ambitious problems are posed that reduce the grid scale; reduce the SGS diffusivities and thereby increase the nonlinearity of the dynamics; and examine both atmospherically forced fluctuations and intrinsic variability arising from instability of large-scale currents. The most energetic forms of the intrinsic variability are mesoscale eddies and even larger-scale, lower-frequency fluctuations generated by instability of the wind-driven currents, and transient, three-dimensional overturning circulations that are generated by instability of the thermohaline circulation. With time an increasingly broad range of scales of motion is therefore being incorporated into the OGCM solutions, thus decreasing the spatial-temporal scales for the requisite SGS parameterizations. Nevertheless, it is inconceivable that a numerical model could incorporate all excited degrees of freedom in the circulation that we estimate as $\mathcal{O}(10^{40})$, if 1 mm and 1 s are taken as the minimum scales, and the whole ocean and 10^4 yr are taken as the maximum scales. Therefore, SGS parameterizations will always be essential elements of an OGCM. The present frontiers for OGCM solutions lie both in fluctuations of decadal or longer periods, coupled with the atmosphere, and in the turbulent behavior of mesoscale currents and eddies.

The fundamental fluid dynamics of oceanic circulation is expressed by the Navier-Stokes equations for the rotating Earth and a compressible liquid (seawater, comprised of water plus a suite of dissolved salts that occur in nearly constant ratio but variable amount — the salinity S) with an empirically determined equation of state. However, since the targets of OGCMs are the large-scale, low-frequency currents, we can choose among several levels of dynamical approximation (Fig. 1; also see Chap. 1):

- The Boussinesq Equations neglect variations of density ρ everywhere in the momentum and mass balances except for the gravitational force, while retaining the full effects of compressibility in the equation of state. This excludes acoustic modes. This is a safe approximation for ocean currents since $\delta\rho/\rho \ll 1$.

- The Primitive Equations make the further hydrostatic approximation in the vertical momentum balance:
$$\frac{\partial P}{\partial z} \;=\; -g\rho\,, \tag{1}$$
where P is the pressure; ρ is the density; z is the local vertical coordinate (parallel to the gravitational force); and g is the gravitational acceleration. This excludes convection (which requires vertical accelerations), and it distorts high-frequency gravity wave dynamics. The hydrostatic approximation is safe as long as $H/L \ll 1$, where H and L are vertical and horizontal length scales characteristic of the solutions. This is true for all OGCM solutions to date, though just barely so. The same condition of small aspect ratio justifies the neglect of Earth's rotation vector $\mathbf{\Omega}$ except for its local vertical projection, *i.e.,* the Coriolis frequency, $f = 2\mathbf{\Omega}\cdot\hat{\mathbf{z}}$ with $\hat{\mathbf{z}}$ local unit vertical vector.

- The Balance Equations further make approximations to the horizontal momentum equations

that are consistent with gradient-wind balance,

$$\frac{1}{\rho_o}\nabla_h^2 P \;=\; \hat{\mathbf{z}}\cdot\boldsymbol{\nabla}_h\times f\mathbf{u}_h + 2\frac{\partial(u,v)}{\partial(x,y)}\,, \tag{2}$$

where ρ_o is the mean density, boldface denotes a vector, the subscript h denotes horizontal component, $\mathbf{u}_h = (u,v)$, and $\mathbf{x}_h = (x,y)$. This is an approximate balance among the divergence of pressure gradient, Coriolis, and centrifugal forces, and it usually is quite an accurate approximation for circulation. This model excludes gravity and inertial waves. There are a variety of particular formulations of balanced models, but among those whose balance relation asymptotically coincides with (2) for small Ro, the differences may not be quantitatively significant.

- The Quasigeostrophic and Planetary Geostrophic Equations are leading-order asymptotic approximations for small Rossby number, $Ro = V/fL \ll 1$ (where V is a characteristic horizontal velocity). They satisfy geostrophic balance,

$$\frac{1}{\rho_o}\boldsymbol{\nabla}_h P \;=\; -\hat{\mathbf{z}}\times f\mathbf{u}_h\,. \tag{3}$$

  The two approximations differ by whether L/R is assumed to be order one or larger, respectively, where $R \sim NH/f$ is the baroclinic deformation radius and N is the buoyancy frequency for the vertical density stratification. The size of R_d is typically in the range 10-100 km, with smaller values at higher latitudes. Each of these models is a subset of the Balance Equations. They suffer from having non-uniform validity in L/R and Ro; from inaccuracy of (3) near the equator where $f = 0$; and, for the Quasigeostrophic model, from the neglect of horizontal and temporal variations in $N(z)$. Nevertheless, these two maximally simplified models are accurate for many particular phenomena in the general circulation and therefore are useful simple models for the theory of ocean currents, hence for the interpretation of OGCM solutions.

When faced with this range of approximations, the early general circulation modelers chose the Primitive Equations because they were confident of the underlying assumptions, and the necessary numerical solution methods were simpler than those required for the Boussinesq or Balance Equations. From a modern dynamical perspective, the alternative choices of either the Boussinesq or Balance Equations could be reasonably defended, but their respective advantages — allowing solutions with H/L not small or having both an intrinsically smoother evolutionary rate (hence permitting a large step size, Δt) and a reduced dynamical phase space within which to interpret the solution, respectively — are unlikely to be enormous ones in most OGCM applications. Another basis for distinguishing among these three models has been their permissible time-step size under the constraint of computational stability for explicit time-integration methods. The permissible step size is larger the greater the degree of physical approximation because of the implied exclusion of faster modes of behavior. This distinction disappear if unconditionally stable, implicit time-integration methods are used (as they partly are for vertical transport processes).

The common basis for an OGCM is the Primitive Equations for a thin fluid layer in spherical coordinates (*i.e.,* replacing the radial coordinate $r = z + a$ by the mean radius of Earth a wherever it appears as an algebraic factor):

$$\begin{aligned}
\frac{Du}{Dt} - \left(f + \frac{u \, \tan\phi}{a} \right) v &= -\frac{1}{a \, \cos\phi} \, \frac{\partial P}{\partial \lambda} + SGS \\
\frac{Dv}{Dt} + \left(f + \frac{u \, \tan\phi}{a} \right) u &= -\frac{1}{a} \, \frac{\partial P}{\partial \phi} + SGS \\
\frac{\partial P}{\partial z} + \frac{g\rho}{\rho_0} &= 0 \\
\frac{1}{a \, \cos\phi} \left(\frac{\partial u}{\partial \lambda} + \frac{\partial v \, \cos\phi}{\partial \phi} \right) + \frac{\partial w}{\partial z} &= 0 \\
\frac{D(T,S)}{Dt} &= SGS \\
\rho &= \rho[T,S,P] \, . \qquad (4)
\end{aligned}$$

Here (λ, ϕ, z) are longitude, latitude, and height; (u, v, w) are the associated velocities; T is the potential temperature (*i.e.,* invariant under adiabatic compression); S is the salinity; and D/Dt is the substantial time derivative,

$$\frac{D}{Dt} = \frac{\partial}{\partial t} + \frac{u}{a \, \cos\phi} \frac{\partial}{\partial \lambda} + \frac{v}{a} \frac{\partial}{\partial \phi} + w \frac{\partial}{\partial z} \, . \qquad (5)$$

Where SGS appears in (4), there are important, small-scale, non-conservative processes. These provide spatial transports and pathways to the dissipation that actually occurs by molecular kinetic processes on scales of $\mathcal{O}(1)$ mm. Implicitly these equations are the result of a low-pass filter at the space-time resolution of the numerical model, with SGS denoting the contributions from the unresolved scales. These equations can be augmented by additional tracer equations similar to those for (T, S), adding whatever chemical reactions are required.

The boundary conditions for an OGCM are comprised of the appropriate kinematic conditions on the normal component of velocity and flux rules for the momentum and tracers. These conditions are particularly simple at solid boundaries, where the normal velocity is zero and tracer fluxes are usually neglected. A bottom stress law is also required there, but this is part of the SGS parameterization (Sec. 2.6.5). Since OGCM domains usually have sides of finite depth as part of their spatial discretization (Sec. 2.5) — unlike the true shoreline in most places — the usual practice is to set the horizontal tangent velocity to zero (*i.e.,* no-slip), although alternative choices of free-slip (no stress) and partial-slip (stress proportional to slip) are sometimes used. These artificial side-wall conditions exert significant influence on OGCM solutions with fine resolution and strong boundary currents. Thus, they are a problematic aspect of the model formulation.

At the upper free surface, $z = \eta(\lambda, \phi, t)$, the kinematic condition is $w = D\eta/Dt$. Current practice is divided between the full use of this condition and the rigid-lid approximation, wherein $w = 0$ at $z = 0$ and the associated sea level is calculated diagnostically from the model's surface pressure, $\eta = P(\lambda, \phi, 0, t)/g\rho_o$. The rigid-lid approximation is based on the assumptions of

$\eta/H \ll 1$ and of slow current evolution compared with surface gravity waves (with a long-wave speed of $\sqrt{gH} \sim 200$ m s^{-1} with $H/L \ll 1$) and long barotropic Rossby waves (with speed $\beta g H/f^2 \sim 100$ m s^{-1}, where $\beta = 1/a\ \partial f/\partial\phi$). A rigid lid is an accurate approximation for most types of currents except for tides and surface gravity waves and for some aspects of response to synoptic weather events. So the choice among the alternative surface kinematic conditions is often made more for computational convenience or efficiency rather than for dynamical content. There are additional momentum and tracer flux conditions at the ocean surface (Sec. 2.2).

When the domain is less than global or full depth, open boundary conditions are required at an internal fluid boundary. There is no fundamentally correct basis for specifying such conditions. However, various rules have been devised that sometimes suffice for the target phenomena of the calculation (Marchesiello et al., 2001). Often these include the various effects of specified inflow, outward wave radiation, restoration of tracers towards their climatological values, and enhanced damping in the neighborhood of the internal boundary (a.k.a., a sponge layer). This is another problematic aspect of OGCM formulation.

2.2 Forcing

The primary forcing of a full-depth, global OGCM is by surface flux of momentum (stress), T (heat), S (water), and other material properties, while side (*e.g.,* rivers) and bottom tracer fluxes may provide secondary forcing but usually are neglected.

The surface stress is caused by the drag by the overlying wind. It is calculated from an empirical wind climatology using bulk regression formulas for stress. This climatology is readily available in several forms and is being systematically improved through satellite wind observations and climatological reanalyses at operational weather forecast centers. In polar regions the stress transmission may be mediated by sea ice. Sea ice changes the drag coefficient in the bulk regression formula for surface stress, and it can inhibit stress transmission to the ocean if ice jams develop. An ice model may be needed to adequately incorporate these effects.

The heat and water fluxes are more problematic, since there is no comparably good climatology for them. Bulk regression formulas can be used together with atmospheric surface climatologies for some locally determined components (*e.g.,* evaporation and sensible and latent heats), but other components are non-locally determined (*e.g.,* precipitation and radiation). Again the presence of sea ice modifies the fluxes, both by blocking air-sea material exchanges and through freezing and melting. Historically the most common practice has been to replace the uncertain flux boundary conditions with restoring terms, *e.g.,*

$$\frac{\partial T}{\partial t} \;=\; \ldots \;+\; \frac{1}{\tau}\,(T_{clim} - T)\,,$$

for the temperature tendency equation for the uppermost model grid level (ditto for S), where T_{clim} is the observed sea surface temperature and τ is a specified relaxation time (usually on the order of

many days). This term can then be diagnostically interpreted as a surface heat flux divided by the grid-cell thickness Δz. This has the seeming virtue of giving model solutions whose T and S fields are close to the observations (but note that the agreement could be complete or the implied surface flux would be zero). Yet OGCM experience shows that the implied fluxes obtained by this method are not physically plausible because of too much small-scale variation and probably even some large-scale bias. These defects are especially severe in S. The physical error in using restoring conditions is that they imply excessively strong local atmospheric feedbacks in which any tendency of the ocean to depart from T_{clim} elicits an atmospheric response that supplies compensating fluxes. On the other hand, choosing the opposite extreme of a specified flux has the dual problems of empirical uncertainty in what to specify and the implied absence of any feedback. The lack of feedback allows the ocean solution to drift far away from climatology due to errors in both the model and the fluxes.

The reality of atmospheric feedbacks is in between these extremes. The flux components that are locally determined do have a greater degree of negative feedback than the non-locally determined ones. An approach that is preferable to either restoring or specified-flux conditions is a mixture of specifying certain components and calculating others with negative feedback forms using an atmospheric climatology from reanalyses as the underlying data base. In most aspects the accuracy in the climatology of atmospheric state variables (*e.g.,* surface air temperature and cloudiness) is better than for the air-sea fluxes. Thus, the former may provide a better empirical basis for specifying surface fluxes than the latter. This approach is a complicated one with many arguable steps, but its resulting OGCM solutions have been found to be better than the alternatives. Ultimately, of course, the fluxes should be self-consistently determined with sea-ice and atmospheric general circulation models.

2.3 Initial Conditions and Equilibrium

The state of the oceanic general circulation is not observed in anywhere near the detail that is required for a complete initialization of an OGCM, nor is it likely to be any time soon. A better global observing system would, however, greatly improve the quality of approximate initial conditions. I believe there is also some utility in retrospective spin-ups using the atmospheric climatology for forcing and data-assimilation methods to provide oceanic constraints. This has not yet been done in a substantial way, and there are interesting open questions about the ways in which the ocean is sufficiently predictable for this approach to yield a unique answer. Some aspects of OGCM solutions, such as wind-driven Rossby waves and upper-ocean thermal fluctuations, do seem to be largely predictable from surface fluxes, but the modes of intrinsic variability are likely to be much less so.

Typical OGCM initial conditions are climatological T and S fields and zero motion. From such a state there is a geostrophic adjustment to the tracer fields within days, followed by boundary, Kelvin, and Rossby wave adjustments to the wind forcing within a few years that leave behind currents that, at least grossly, resemble the long-time equilibrium state. The true equilibrium state

occurs only after thousands of years when advection and SGS transport have redistributed the T and S fields consistent with the OGCM problem as posed. Unless approximately correct tracer fields are given as initial conditions, an OGCM solution will differ greatly from its equilibrium state after an integration of only several years. Scientists who wish to avoid the costly computations to reach full equilibrium do bear the burden of demonstrating that shorter integration times do not excessively bias their solutions. At present it is computationally infeasible to integrate a global OGCM to an equilibrium state using mesoscale resolution.

Another obvious approach to initialization is by bootstrapping (*i.e.,* using one equilibrium OGCM solution as an initial condition for another, differently-posed problem). We might expect this method to be helpful in shortening the approach to equilibrium if the family of solutions were all sufficiently close to each other. The common experience to date, however, is that this method is rarely cheaper than restarting from a stratified state of rest when the goal is to closely approach an equilibrium state.

2.4 Numerical Methods

The computational algorithms that have been used for OGCMs have mostly been rather simple ones, as presented in Bryan (1969) and by others with minor variations. They are a finite-difference discretization of (4)-(5), using centered, nearest neighbor differences that are second-order accurate in the grid spacing for uniform grids (the usual choice in (λ, ϕ)) and formally first-order for the (usually weakly) non-uniform vertical grids with finer resolution in the more stably-stratified upper ocean. The grids are staggered in their distribution of the dependent variables, using one of several alternative schemes, with the B- and C-schemes the most common. The spatial difference operators are integrally conservative for tracer content and variance and for kinetic energy. Near the poles extra smoothing is required if the grid spacing becomes very small, as it does on a uniform longitude-latitude grid.

The time-stepping is by a mixture of first- and second-order accurate procedures, with time-splitting often used to solve separately for the SGS vertical mixing by an implicit algorithm that is computationally stable for arbitrarily large SGS vertical diffusivity and to solve for everything else by an explicit algorithm. If the full free-surface kinematic condition is used, then it too is handled though a time-splitting procedure. In these situations the time step size Δt is limited by CFL stability conditions for advection, internal gravity and barotropic Rossby wave propagation, and SGS lateral transport. Over a rather wide range of spatial grid size, $\Delta t = \mathcal{O}(1)$ hr. Therefore, integrating for $\mathcal{O}(10^3)$ yr to approach equilibrium requires $\mathcal{O}(10^7)$ time steps or more.

The coarsest spatial grids used in global OGCMs have $\mathcal{O}(10^5)$ grid points, corresponding to a horizontal spacing of hundreds of kilometers and a vertical spacing of hundreds of meters. To be adequate for mesoscale eddies, the grid resolution must have horizontal spacing appreciably finer than the internal deformation radius, R. This requires a scale of $\mathcal{O}(10)$ km (also see Sec. 3.2), which increases the size of a global grid to at least $\mathcal{O}(10^8)$ points. At present it is still infeasible

to combine full mesoscale resolution with full equilibrium in a single global calculation, although it will likely become possible within the next decade with faster computers. Since this computer power probably will be achieved only with substantial parallelism, there is a considerable incentive for creating suitably structured OGCM code architectures, and this demands quite sophisticated knowledge.

Often a shortcut for reaching equilibrium can be taken for coarse-resolution OGCMs by acceleration. This is a time-stepping technique in (4) with a larger Δt for (T, S) than for (u, v), and a further increase in Δt for the deep tracers. The rationale is that the CFL constraint is usually most severe on (u, v) through the SGS horizontal momentum diffusion and the fastest waves, whereas the constraint for tracers is set by their slower SGS lateral transport and advection (which decrease with depth). Since deep tracers are the slowest solution components to approach their equilibrium values, this acceleration technique can reduce the integration time by a factor of $\mathcal{O}(100)$. If the OGCM approaches a steady solution under steady forcing, then this distortion of the transient dynamics causes only a transient error. Even with periodic seasonal forcing, acceleration leads to a valid equilibrium solution if followed by a synchronous integration with uniform Δt for $\mathcal{O}(10)$ yr, to allow the seasonal cycle to equilibrate. No doubt this particular technique has a limited range of validity in model resolution and solution transience, but more robust acceleration methods are well worth seeking because of the high computational cost of calculating OGCM equilibria.

Since more sophisticated numerical methods than those described above are now well established in other computational contexts, a spate of numerical developments for OGCMs is likely to occur soon. Some of the interesting areas of development are higher order spatial and temporal discretizations; advection operators not so prone to creating erroneous extrema; fuller temporal implicitness to escape physically unimportant computational stability limits; more efficient procedures for solving for a reference-level $P(\lambda, \psi, t)$ in the vertical integration of the hydrostatic relation, via the barotropic streamfunction, rigid-lid surface pressure or free-surface elevation; and local grid refinement or nesting to allow a regional focus with less physical uncertainty and numerical error in the open-ocean side boundary conditions. The model that I most closely work with these years (Regional Oceanic Modeling System, ROMS) embodies many algorithmic advances over those used in standard, community OGCMs (Shchepetkin and McWilliams, 2005, 2006).

The governing equations (4)-(5) are physically equivalent in any coordinate transformation, but uniform grids in different coordinate systems imply different discretizations of the equations. One useful application is to achieve a more uniform tiling of the sphere in the horizontal coordinates than in a regular latitude-longitude grid. This improvement is most important near the north pole where $\Delta\lambda \to 0$. Another potentially useful application is through transformation of the vertical height coordinate z to either a potential-density or a topography-following (*i.e.,* σ) coordinate. Advantages of a potential-density coordinate are a natural concentration of resolution in the pycnocline where vertical gradients are often largest; the simplification of the conservative nonlinear terms in (4)-(5) involving only the horizontal velocity; and a relative ease in assuring integral conservation properties for the discretized, isopycnally-oriented SGS operator forms (although this has also been achieved satisfactorily with other coordinates; Sec. 2.6.2). Disadvantages are an

uncontrollable sparseness of resolution in weakly stratified regions, such as in boundary layers and convective sites; errors in implementing the equation of state associated with its nonlinear form of compressibility so that globally defined density or potential density surfaces are not uniformly accurate in representing the static stability; and a greater complexity in specifying the discrete diapycnal SGS operator forms. Advantages of a topography-following coordinate are a more accurate representation of the bottom kinematic boundary condition and bottom boundary layer SGS mixing. A well known disadvantage is the error in the horizontal pressure gradient force where the topography is especially steep (though there may be similar, albeit less obvious, errors in other coordinate systems). Another potential disadvantage is the vanishing grid spacing as the depth becomes very shallow at the ocean margins, with a possibly severe constraint on the time step size for computational stability. In my opinion no vertical coordinate choice is clearly the superior one. Probably the more important choices are for the discrete operators that arise within a given coordinate system.

2.5 Domain Geometry

The shape of an ocean basin is defined by its bottom topography, including its intersection with the top surface, the coastline. Topography has a profound influence on the direction of currents, especially near the bottom. The reason for this is the approximate material conservation of potential vorticity, whereby a change in the thickness h between a deep interior isopycnal surface and the bottom implies a compensating change in the fluid vorticity that acts to turn the fluid trajectory toward a path of constant f/h.

It is far less certain, however, when and where topography fundamentally controls the existence and strength of the large-scale currents. The currents are strongest in the upper ocean where they are accelerated by internal pressure gradient forces, closely related to (T, S) distributions through hydrostatic balance and the equation of state. Momentum balance against this acceleration can be provided either internally by large-scale advection and SGS transport or by topographic effects. The important topographic effects are form stress (*i.e.,* integrated horizontal pressure force on the bottom), boundary-layer drag, and hydraulic control (*i.e.,* throughflow limited by a critical Froude number, where the velocity equals the gravity-wave speed). This competition can be posed conceptually as a comparison of different model solutions with either simpler, smoother topography or rougher, more complex topography. While the desire for geographical realism favors the latter, achievement of computational accuracy favors the former (*i.e.,* accurate numerical solutions require smoothness near the grid scale), and the choice of numerical algorithms for topography may be quite important in determining the balance point between these competing goals. There is no satisfactory resolution of these issues at present, and the common practice is one of trial and error. Increasing the grid resolution allows the incorporation of finer topographic features. This diminishes the scope of the ambiguity in specifying topographic smoothness, although the true topography in the oceans remains rough on all conceivable OGCM scales.

Some aspects of topographic influence must be represented in the SGS parameterizations: the

bottom boundary layer, coastal shoaling, small-scale roughness, and, probably, hydraulic control (I am not aware of any OGCM solutions that achieve this state in their resolved dynamics, although the governing equations admit the possibility). At least part of the effects of form stress and impedance by constricting straits are resolved dynamical processes.

Constricting straits can limit throughflow, either by boundary stress or hydraulic control. In OGCM solutions a current through a strait whose width is too close to the grid scale will have a primarily viscous dynamics. A small width probably exaggerates the boundary stress and precludes the inertially controlled dynamics of hydraulic control. This presents a modeler with the temptation to artificially widen or deepen the channel to compensate for these biases, but this is an essentially arbitrary choice. The two most important straits in the global ocean are the Drake Passage and the Indonesian Archipelago, and both have large throughflows. Coarsely resolved OGCM solutions have about the same transport as observed when these straits are artificially widened. Straits occur in all sizes, of course, and some will remain part of the SGS specification at all foreseeable resolutions. Probably the most important of these is the Strait of Gibraltar, whose outflow of salty, Mediterranean seawater has significance in the S budget of the North Atlantic Ocean; it is likely that this flow is under hydraulic control part of the time. There are analogous difficulties with flow over sills and ridges whose size is too close to the grid scale. A notorious example is the flow of deep seawater from the Greenland Sea into the Atlantic across the Icelandic Ridge.

2.6 Parameterizations

The art of parameterization is to augment the resolved dynamics in (4) with mathematical operators that accomplish the necessary physical effects by unresolved SGS processes, all of which involve turbulence and thus do not have complete analytic theories to make use of. I believe it is impossible to make a parameterization rule that is entirely correct, in the sense that it will yield the same answer as in a model that fully resolves the process. Therefore, a hypothesis must be declared about what the minimum necessary effects are. Then, after finding a suitable operator that satisfies this hypothesis, any free parameters are chosen to either achieve some quantitative effect in an OGCM solution or match independent data about the process — both, if possible. The most common parameterization hypothesis about turbulent processes is that they mix material properties, hence the most common operator form is eddy diffusion (*e.g.,* by spatial Laplacian operators) with an eddy diffusivity coefficient as the free parameter.

We should be humble about of our ability to represent turbulent processes. So, a guideline for choosing a good parameterization is to keep it as simple as possible, with as few free parameters as possible, consistent with achieving both the hypothesized effect and a significant impact on the solution. Nevertheless, for an OGCM there are many needed effects associated with many different SGS processes, so many different parameterization forms are involved.

Material transport in the oceans is strongly constrained by the iso-surfaces of entropy, which are locally tangent to iso-density surfaces. Momentum transport is less constrained because of the

pressure-gradient force.) In a stably-stratified region, gravitational work is required to move matter across surfaces of neutral buoyancy (*i.e.,* isopycnal surfaces). Hence transport along these surfaces is much more efficient than across them, with an observed ratio of cross-isopycnal (*i.e.,* diapycnal) to isopycnal eddy diffusivities of about 10^{-8} in the oceanic thermocline. The principal agents of turbulent isopycnal tracer flux are mesoscale eddies, which crinkle the basin-scale isopycnal surfaces without disrupting their stable vertical ordering. The agents of diapycnal tracer flux are micro-scale motions that can cause overturning and fragment the surfaces. Within and near the surface and bottom boundary layers, where the density stratification is weak, this constraint is lifted and micro-scale transports are much more efficient than in the interior.

2.6.1 Lateral Momentum Transport

For the general circulation the dominant mechanism for lateral momentum transport is by mesoscale eddies acting through the horizontal Reynolds stress, $\overline{\mathbf{u}_h' \mathbf{u}_h'}$. This process can either be wholly parameterized or be partially resolved in an OGCM. The common parameterization is horizontal eddy diffusion, with an eddy viscosity $\nu_h \geq 0$, although hyperdiffusion (*i.e.,* an iterated Laplacian operator) is sometimes used to strengthen a marginally resolved instability process such as Gulf Stream meandering. The value of ν_h depends upon the grid size. It must be large enough to resolve the viscous boundary layers of width $\sim (\nu_h/\beta)^{1/3}$ and to suppress nonlinear computational instability on the grid scale (*i.e.,* a grid Reynolds number, $Re = V\Delta s/\nu_h$ cannot be large). Fundamental symmetry principles about the nature of a stress divergence imply that the operator must have additional terms beyond a simple Laplacian operator in a spherical domain (Wajsowicz, 1993). A similar consideration applies to spatially non-uniform or anisotropic eddy viscosities that are sometimes used when the grid spacing has the same attributes (Large et al., 2001; Smith and McWilliams, 2003).

There is a well-known counter-example for this parameterization, which prompted Victor Starr to talk about "negative eddy viscosity". It is the counter-gradient eddy momentum flux that occurs in the core of a broad (*i.e.,* with $L/R \gg 1$), baroclinicly unstable current, such as the Antarctic Circumpolar Current (Chap. 4). This has led some to suggest replacing lateral eddy viscosity with potential vorticity diffusion (Chap. 3, Sec. 3.5), although this has not yet been implemented in an OGCM. Furthermore, since the momentum flux need not be related to the local large-scale flow, as with Rossby wave propagation through a region, an eddy diffusion form may not always be valid. Analyses of eddy-resolving OGCMs indicate the resolved horizontal Reynolds stress divergence patterns are locally much different from the eddy viscosity parameterization, especially near mid-latitude western boundary currents where they are largest. With fine enough grid resolution and small enough ν_h in an OGCM, these confounding behaviors can become part of the resolved dynamics, and an eddy viscosity parameterization may suffice.

2.6.2 Isopycnal Material Transport

The traditional parameterization for lateral tracer transport is horizontal eddy diffusion, but this violates the constraint of tracers mostly staying on isopycnal surfaces, with $\overline{\mathbf{u}c'}$ nearly perpendicular to $\boldsymbol{\nabla}\overline{\rho}$ (here c is any tracer concentration). The parameterization by Gent and McWilliams (1990) that is isopycnally oriented and integrally adiabatic (*i.e.,* without interior sources or sinks of any material property that alters its inventory on isopycnal surfaces) has had quite beneficial effects on OGCM tracer distributions and fluxes. In addition to tracer diffusion along isopycnals, there is an incompressible eddy-induced transport velocity (also see Chaps. 3-4). Its horizontal component is defined by

$$\mathbf{u}_h^* \equiv \left(\frac{\partial \overline{z}}{\partial \rho}\right)^{-1} \overline{\frac{\partial z'}{\partial \rho}\mathbf{u}_h'}\,, \tag{6}$$

where z is height of an isopycnal surface and the overbar is an average over the mesoscale on that surface. $\mathbf{u}^*$ combines with the large-scale $\mathbf{u}$ as the large-scale Lagrangian velocity that advects the large-scale tracers. $\mathbf{u}^*$ also advects the isopycnal surface itself, thereby causing vertical transport of momentum, as in isopycnal form stress, and depletion of available potential energy, as in baroclinic instability. In present OGCM implementations, both $\mathbf{u}^*$ and the isopycnal mixing are represented as eddy diffusion of isopycnal layer thickness and tracers. The originally suggested parameterization form for the eddy-induced velocity is

$$\mathbf{u}_h^* = -\frac{\partial}{\partial z}\left[\kappa_i \mathbf{L}_h\right], \quad w^* = \boldsymbol{\nabla}_h \cdot \left[\kappa_i \mathbf{L}_h\right], \tag{7}$$

although variant forms have since been suggested by others. Here $\mathbf{L}_h = -\boldsymbol{\nabla}_h\rho \Big/ (\partial\rho/\partial z)$ is the slope of the isopycnal surface. The eddy diffusivity, $\kappa_i \sim 10^3$ m^2 s^{-1}, can be identified with the rate of dispersion of neutrally buoyant floats in the ocean. So far, κ_i has been used in coarse resolution OGCMs with essentially no grid-size dependence in its value. Even in fine resolution calculations that partially resolve the mesoscale eddies, there is benefit to using this parameterization with a smaller κ_i, if only to avoid false diapycnal flux. Since mesoscale variability is strongly inhomogeneous in the ocean, it seems likely that κ_i should also be variable. Some people have suggested flow-dependent rules for κ_i based on linear baroclinic instability theory, and currently these rules are being explored.

An important modification to the preceding eddy parameterization scheme is made near the boundaries, especially near the top surface where the PBL is. The modification is to abandon the interior assumption of quasi-adiabatic transport and isopycnal orientation for the eddy fluxes in favor of diabatic transport and along-boundary orientation. In particular this implies that $\mathbf{u}^*$ be parallel to the boundary (as it must be by a tracer conservation principle) but generally non-zero (unlike in some OGCM implementations). Such a scheme is proposed in Ferrari and McWilliams (2006).

If one assumes a simplified $\rho[T, S, P]$ and neglects SGS terms in (4), then the hydrostatic form

of Ertel potential vorticity is

$$\begin{aligned} q &= \left(f(\phi) + \frac{1}{a\,\cos\phi}\left[\frac{\partial v}{\partial \lambda} - \frac{\partial (u\,\cos\phi)}{\partial \phi}\right]\right)\frac{\partial \rho}{\partial z} \\ &- \frac{1}{a\,\cos\phi}\frac{\partial u}{\partial z}\frac{\partial \rho}{\partial \lambda} + \frac{1}{a}\frac{\partial v}{\partial z}\frac{\partial \rho}{\partial \phi}\,, \end{aligned} \tag{8}$$

With mixing q is conserved along parcel trajectories that lie on isopycnal surfaces. (This is also true in the other models in Fig. 1 with alternative definitions for q.) If mesoscale eddies are strong enough, they sometimes can mix, or homogenize, large-scale q (Chap. 3), although they do not always. A large-scale approximation to q is $f\rho_z$, and there are some regions in the ocean where $f\rho_z$ quantity is observed to be nearly uniform along isopycnal surfaces (*e.g.,* Chap. 3, Fig. 25). Also, at least in zonally symmetric channel flows, eddy potential vorticity fluxes may be more uniformly down-gradient than eddy thickness fluxes. This suggests that isopycnal potential-vorticity mixing is a possible parameterization hypothesis. It would be expressed as a composite of the SGS terms in the momentum, T, and S equations in (4), and as such it must be reconciled with them in a way that does not involve double counting of processes. An eddy diffusion of potential vorticity should avoid the fallacy of generating a large-scale flow from a resting stratified state; this suggests that the diffusivity has to be flow dependent. For those who believe that a resting state is physically unrealizable because nature always contains many sources that excite currents, this consideration may be considered irrelevant. Since the usual methods for solving (4)-(5) do not involve an equation for q explicitly, a different method would be required. There are thus significant challenges to be overcome in implementing a q-mixing parameterization in an OGCM, and potential vorticity mixing may prove to be more useful as a theoretical concept than as a practical parameterization form.

2.6.3 Surface Boundary Layer and Surface Gravity Waves

In the surface planetary boundary layer (PBL), small-scale turbulence is relatively strong because of shear and buoyancy instabilities resulting from the surface fluxes, hence $\overline{w'\mathbf{u}'_h}$ and $\overline{w'c'}$ are much larger than in the interior (Chap. 2). In the default SGS form, the PBL is implicitly contained within the top grid cell of an OGCM since there are no elevated diffusivities in the grid interior. An essential extension beyond the default form is to increase the vertical SGS fluxes where the density stratification is gravitationally unstable (*i.e.,* with a positive vertical gradient in potential density), mimicking the convection that cannot be dynamically resolved in (4). This is often done either by convective adjustment (a minimal vertical rearrangement of tracers until stable stratification is achieved) or by a substantial enhancement of the vertical diffusivities in the unstable region. Insofar as the convection arises from an upward surface buoyancy flux — as it usually does — the PBL extends from the surface throughout the depth interval of adjustment or enhanced mixing. In this situation an explicit boundary layer model for the PBL transport is preferable to a local mixing rule.

The most commonly used PBL model types in OGCMs used to be either bulk mixed-layer

models or single-point, moment-closure turbulence models. Large et al. (1994) reviews the usage of oceanic PBL models and proposes a K-profile parameterization (KPP) that has more recently become widely used. KPP does not impose such a strong constraint on the boundary layer profiles of large-scale variables as does a mixed-layer model, and it escapes the dubious spatial locality assumption of moment-closure models. It also includes counter-gradient buoyancy and fluxes in convective situations. The KPP hypotheses are

1. The boundary layer thickness h maintains a bulk Richardson number, $Ri_b = -gh(\Delta\rho)\Big/(\Delta\mathbf{u})^2$ (where Δ indicates the difference across the boundary layer), at a critical $\mathcal{O}(1)$ value.
2. The diffusivity profile smoothly joins with the Monin-Obukhov form near the surface and hoins with the interior form at the outer edge of the boundary layer.

In the several assessments of its performance in OGCMs to date, KPP does fairly well. It is important that PBL vertical mixing not occur simultaneously with isopycnal tracer transport (which presumes a strongly stable stratification) in an OGCM, or else the exchange between the boundary layer and the interior will be too rapid. Accordingly, a rule is used that turns off κ_i where $z \geq -h$ or $\boldsymbol{\nabla}_h\rho\big|\Big/\rho_z$ is too large.

As yet no OGCM includes several SGS effects of surface gravity waves that probably are important for large-scale flows under some conditions. One effect is enhanced mixing by breaking waves near the surface and by wave-driven Langmuir cells throughout the PBL. Another effect is that the wave-averaged dynamics contain extra terms in both the horizontal momentum and tracer equations in (4). These terms are proportional to the mean Lagrangian velocity of the waves, the Stokes drift, and their effect is somewhat analogous to the mesoscale-eddy $\mathbf{u}^*$ term (Sec. 2.6.2). Furthermore, averaging over the waves yields extra terms in the surface kinematic and pressure boundary conditions are related to the divergence of the Stokes-drift transport and the vertical velocity variance of the waves, respectively (Chap. 2).

2.6.4 Interior Vertical or Diapycnal Mixing

The default SGS parameterizations for diapycnal momentum and tracer transports in the oceanic interior (*i.e.,* $\overline{\mathbf{u}'\mathbf{u}'_h}\cdot\boldsymbol{\nabla}\rho$ and $\overline{\mathbf{u}'c'}\cdot\boldsymbol{\nabla}\rho$ are eddy diffusion, with uniform $\nu_v \sim 10^{-4}$ m^2 s^{-1} and $\kappa_v \sim 10^{-5}$ m^2 s^{-1}. Not uncommonly, these values are made to increase with depth in the deep ocean, which has some observational support. Such a tracer diffusivity is inherently non-adiabatic, in the sense defined above, and it implies a breaking of the isopycnal surfaces. These are usually represented as a vertical flux, since this direction is nearly perpendicular to isopycnal surfaces in most places. (Isopycnal slopes are typically $\mathcal{O}(10^{-4})$.) For a given, non-uniform vertical grid, a sufficiently large vertical eddy diffusivity is needed to dominate the implicit numerical diffusion arising from discretization errors. Therefore, often larger (ν_v, κ_v) values are chosen for coarser

vertical grids. There is a continuing controversy over whether the global oceanic circulation is consistent with the small diffusivity values above, or whether "missing mixing" processes must be found. My opinion is that the case for missing diapycnal mixing has not yet been conclusively made for processes in the upper ocean since OGCM solutions with comparably small κ_v values do not have clear discrepancies with observations. OGCM solutions probably do require larger κ_v values in the abyssal ocean to match observed tracer distributions, although this has not yet been clearly demonstrated.

There are various small-scale processes, in addition to convection, that make the interior diabatic mixing spatially and temporally non-uniform and sometimes elevated above the default values. Most notable among these processes are stratified shear instability, breaking internal waves, and double diffusion caused by the larger molecular diffusivity of T than of S. Shear instability influences the equatorial undercurrent and thermocline profiles in OGCM solutions using a parameterization where (ν_v, κ_v) vary inversely with the gradient Richardson number, $Ri_g = N^2 \Big/ (\partial \mathbf{u}/\partial z)^2$. Demonstrations of potentially substantial consequences on the abyssal tracer distributions have been made for a κ_v varying inversely with N, and for double diffusion with unequal κ_v values for T and S. There even seems to be a shows moderate sensitivity of the meridional overturning circulation and heat flux to the double diffusion parameterization. The nonlinearity in $\rho[T, S, P]$ also allows for locally enhanced vertical transport through thermobaric and cabbeling instabilities. The effects of $\rho[T, S, P]$ nonlinearity are present in principle in OGCM solutions that have enhanced vertical diffusivity in the presence of convective instability, but their significance has not been broadly assessed.

2.6.5 Bottom Boundary Layer and Gravity Currents

There is an analogous PBL at the ocean bottom, driven principally by boundary stress without any significant buoyancy flux. A primary effect of the bottom PBL is to provide a drag force on the adjacent flow, as in a simple Ekman layer. Usually in OGCMs this is represented as a boundary stress proportional to $\mathbf{u}$ or $|\mathbf{u}|\mathbf{u}$, acting only in the deepest grid cell. Obviously, an explicit PBL model, of the types discussed above, could be used at the bottom. Some people have argued for the possible significance of tracer transport parallel to the boundary by PBL turbulence. This implies a diapycnal flux for any isopycnal surfaces intersecting the bottom, which locally diminishes the impedance to diapycnal exchanges. This effect has not yet been examined in an OGCM, there has been a demonstration that plausible solutions in simple domain geometry can be obtained by limiting κ_v to be non-zero only near the sides.

Gravity currents are down-slope, bottom flows with a density greater than their surroundings at the same level. This makes gravity currents doubly turbulent, due both to the stress against the bottom and to gravitational instability compared to their downstream environment. Therefore, they efficiently entrain and mix with the ambient fluid as they flow. Gravity currents occur where convection over a slope penetrates to the bottom or dense water overflows a continental shelf or a sill, and they will continue either until entrainment quenches the density anomaly, geostrophic

adjustment turns the flow to be across the slope (though bottom stress keeps the flow turbulent and allows a continuing, albeit slower, downslope progression), or the bottom of the slope is reached. Several sites in the global ocean have significant water mass flows in gravity currents. These include the Mediterranean outflow, the Denmark Straits overflow, and outflows from the Antarctic coastal shelves. The usual practice in OGCMs is to ignore this process, and this is probably unwise. Recently several parameterizations have been proposed for bottom gravity currents (Beckmann and Döscher, 1997), and better ones are actively being sought.

2.6.6 Topographic Effects

The common practice with OGCMs is to include only the effects of topography that are resolved on the model grid, as discussed in Sec. 2.5 above. Here we consider some additional SGS effects that require parameterization.

Small-scale topography influences large-scale circulation. The most direct possibility is through a turbulent rectification process wherein mesoscale eddies above topography cause a form stress that drives large-scale currents along large-scale contours of f/h, where h is the effective vertical scale above the bottom of the affected currents. This may be a significant effect on continental slopes by driving barotropic, cyclonic currents around the rim of the basin. I believe that SGS form stress is a qualitatively important effect to include in OGCMs, although its strength, its vertical structure, and its relationship to the resolved form stresses all need further clarification. A less direct effect of topographic roughness is its tendency to make the vertical structure of mesoscale eddies more surface intensified, with implications for their transport properties in the general circulation. Large-scale currents over rough topography can generate gravity waves, especially stationary lee waves, that propagate vertically into the interior, depositing their momentum and enhancing diapycnal mixing where they break and dissipate. This is an important mechanism for the atmospheric general circulation, and recent observations indicate the occurrence of the process in the oceans as well. Finally, topography on the scale of the bottom boundary layer generates local secondary circulations that may substantially alter the vertical momentum flux and diapycnal mixing rate. No SGS proposal has yet been made to account for this effect.

2.6.7 Rivers and Marginal Seas

The common practice for OGCMs is to neglect river inflows and SGS exchanges with marginal seas. Restoring terms, if used, may indirectly contribute some of these otherwise missing effects. If restoring terms are not used for the surface fluxes, then lateral tracer restoring conditions could be used in places with rivers or significant marginal sea exchanges, in the form of an open boundary condition.

It is better physics to have flux boundary conditions for river inflow, with the inflow specified either from data or a land hydrology model. Then the river inflow appears as just another compo-

nent of the surface water flux for that location. The exchanges with SGS marginal seas or straits (*e.g.,* Bering and Gibraltar) could be specified as lateral flux conditions, determined either from data or from coupling with a local model of their circulation.

3 Solutions

3.1 Global Solutions

In this and the following section, several common diagnostic measures are presented from two examples of modern OGCM solutions: a global equilibrium solution with relatively coarse horizontal resolution and an Atlantic basin solution with relatively fine resolution.

The global solution is one reported in Gent et al. (1998), which was partly motivated by the development of the Climate System Model by NCAR. The model resolution is 2.4^o in longitude, 1.2-2.4^o in latitude (finer in tropical and polar regions), and 45 levels in the vertical with a vertical spacing expanding with depth from 12.5 to 250 m. Its surface forcing is a mean annual cycle with a combination of specified fluxes and feedback/restoring relations as described in Large et al. (1997). The model uses the isopycnal tracer transport parameterization and the KPP boundary layer and interior vertical diffusivity parameterizations described above. The calculation is carried to equilibrium using the acceleration technique, with a final 17 years of synchronous integration. The solution behavior is presented here primarily through figures from Gent et al. (1998), with only limited discussion of their interpretation and accuracy.

The time-mean surface currents in Fig. 2 show strong westward currents near the equator, eastwards currents around Antarctica, and western boundary currents in the sub-tropical and sub-polar gyres. The interior, extra-tropical currents exhibit Ekman-layer turning from the surface wind stress, to the right (left) in the northern (southern) hemisphere.

The time-mean horizontal transport streamfunction in Fig. 3 shows weak barotropic flow near the equator, anti-cyclonic sub-tropical gyres in all basins, cyclonic sub-polar gyres in the northern basins, and the Antarctic Circumpolar Current. Time series of the annual cycle of transport in the Antarctic Circumpolar Current, Indonesian Throughflow, Kuroshio, and Gulf Stream are shown in Fig. 4.

The time-mean, global meridional transport streamfunction is in Fig. 5 (left). It shows shallow, wind-driven (Ekman) cells near the equator and in the northern sub-polar region, a deep wind-driven Deacon Cell in the Antarctic Circumpolar region, a strong northern thermohaline cell with sinking mostly in the North Atlantic and extension into the southern hemisphere at middle depths, and a weaker Antarctic thermohaline cell that extends along the bottom into the northern hemisphere. Fig. 5 (right) is the sum of this meridional transport plus the time-mean, zonally integrated eddy-induced transport from (7). Its largest effect is a near cancellation of the Deacon Cell except

in the diabatically forced region in the upper ocean.

Time- and horizontal-mean vertical profiles of $T(z)$ and $S(z)$ are in Fig. 6, both from the model solution and from a hydrographic climatology. These profiles show a sharp thermocline and halocline in the upper ocean and more uniform water properties in the deep ocean. $S(z)$ shows a shallow maximum and an intermediate-depth minimum.

Time-mean, longitude-integrated meridional transports of heat and freshwater are shown in Figs. 7-8, both from the model solution and from several empirical estimates. The heat transport is poleward in both hemispheres, with its peaks near $\pm 20^o$. In the southern hemisphere, the heat transport becomes very small across the Antarctic Circumpolar Current, because of the partially canceling effect there of the meridional overturning by the eddy-induced circulation (*cf.,* Chap. 4). The model heat transport is within the uncertainties of the empirical estimates. Although the general shapes of the model and empirical water transport curves agree fairly well, estimating the uncertainties is more problematic than for heat.

3.2 Basin Solutions

The basin solution is one reported in Smith et al. (2000). It was partly motivated by the World Ocean Circulation Experiment Community Modeling Effort for comparing high-resolution OGCM solutions. The model domain is the tropical and North Atlantic basin, between 82^o W and 17.2^o E (Hudson Bay excluded) and 20^o S and 72.6^o N; it also includes the eastern part of the Gulf of Mexico mapped into Africa and part of the Mediterranean Sea. Its horizontal grid is in Mercator coordinates with a resolution of 0.1^o at the equator, and it has 40 vertical levels, varying smoothly from 10 m at the top to 250 m at depth. The forcing is by daily winds (1985-1995), heat flux as in Barnier et al. (1995), and surface restoring to mean monthly S from Levitus (1982). Lateral buffer zones with T, S restoring are used along all open boundaries. The solution is spun up from climatological T, S and $\mathbf{u} = 0$, and the solution averages below are for years 6-10.

The time-mean currents are shown in Fig. 9 at two levels, one near the surface and the other at a middle depth. Near the surface, the western boundary currents have a similar pattern to those in the coarse-resolution solution (Fig. 2), except they are faster and narrower here, especially in the off-shore Gulf Stream. At the middle depth, the western boundary current is southward and is part of the thermohaline circulation seen in Figs. 5 and 11. It shows complex standing eddies in the off-shore Gulf Stream region and near the Grand Banks.

The time-mean horizontal transport streamfunction is in Fig. 10. Compared to Fig. 3, it shows stronger recirculation cells near the western boundary and a greater tendency for following the topographic slopes of the basin. The time-mean meridional transport streamfunction is shown in Fig. 11. Its overall amplitude is similar to the global thermohaline circulations in Fig. 5, although the patterns are somewhat different, particularly with respect to the sub-tropical maximum in the basin solution. This circulation component is substantially influenced by the lateral buffer zones

near the northern and southern boundaries.

The time-mean sea surface elevation is in Fig. 12. It shows the broad, geostrophic, sub-tropical and sub-polar gyre circulations, and the enhanced recirculation cells near the western boundary. A zonal pressure gradient is evident along the equator, which drives the eastward Equatorial Undercurrent.

A plot of instantaneous sea surface temperature is in Fig. 13. In addition to the broad-scale pattern imposed by the climatological surface heating, it shows meanders and filaments associated with advection by the mesoscale eddies and boundary currents.

The time-mean sea level variability is in Fig. 14. It shows higher values where the mean currents are stronger, but the spatial extent of such regions is broader (cf., Figs. 9 (left) and 12). Note in particular the elevated eddy energy along the Azores Current and the North Atlantic Drift. Wavenumber-frequency spectra of sea-surface elevation in the Gulf Stream region are in Fig. 15, both from the model solution and from altimeter measurements. In the mesoscale bands, the OGCM variability matches quite well the observations. On the longest scales the model variability seems slightly higher, and at fine scales the model variability is clearly less.

The horizontal pattern of S at a middle depth near the Mediterranean is in Fig. 16. The outflow water, diluted until it achieves neutral buoyancy with its surrounding, is being spread and mixed by mesoscale eddies that are qualitatively similar to the observed Mediterranean Eddies (Meddies), although they are only marginally resolved in this solution.

3.3 Spatial Resolution

From the perspective of a computational mathematician, there is nothing mysterious about the influence of the spatial grid spacing in a numerical calculation: in a given problem, once the resolution is fine enough for the solution to be smooth on the grid scale, the solution converges with increasing resolution according to the order of the discretization method. For oceanographers the influence of resolution in OGCMs often has been a matter of confusion, and public discussions have often generated more heat than light. There are at least three reasons why the oceanographic issues go beyond the computational mathematical dictum:

- It is common practice to change the problem with the resolution, both by decreasing at least some of the eddy diffusivities (the lateral viscosity, in particular) to its computational-stability limit and by adding finer scales to the forcing and domain geometry.
- Qualitative changes in the solution behavior occur with resolution — mainly due to changing the eddy diffusivity — as instability thresholds are passed. The most striking change is the emergence of mesoscale eddies, but this actually involves a suite of thresholds for the many different currents in the general circulation.

- The general circulation has many aspects in its behavior, and no complete understanding exists yet for how different features differently depend on resolution and each other.

There are remarkably few published studies of the influence of resolution in OGCMs, and more certainly would be worthwhile. The evidence in hand suggests that it is relatively unimportant for those solution properties, such as tracer fluxes and water mass distributions, that are simulated reasonably well in OGCMs without resolved mesoscale instabilities (*i.e.,* with horizontal grid spacings $dx > 50$ km); Covey (1995). In such models, the boundary currents typically are too weak and broad but are not as incorrect in their transport; the eddy-driven western recirculation gyres are missing; and the equatorial currents are too weak and broad except when the meridional resolution is locally refined to a scale smaller than 50 km.

Once the grid is fine enough for eddies to arise, the resolution seems to be extremely important — up to an as yet poorly determined threshold at least as small as 10 km — to calculate mesoscale eddies and boundary currents credibly. For eddy-resolving models, resolution convergence has not been demonstrated and remains an important open issue. However, several recent OGCM solutions for the Atlantic with especially high vertical or horizontal resolution do appear to have achieved certain correspondences with the observations lacking at lower resolution (*e.g.,* eddy kinetic energy density, Gulf Stream separation site and off-shore path, and meridional heat flux), including the one shown in Sec. 3.2. On the other hand, recent further exploration of the sensitivities of eddy-resolving solutions by Bryan et al. (2006) show both delicacy and bias, *e.g.,* for the Gulf Stream path after it separates from the western boundary (Fig. 17). And some features have not yet been seen in OGCM solutions that are present in idealized models at very fine resolution (Chap. 3); examples of this are the instability of the western boundary current before separation, an intrinsic low-frequency variability on decadal periods, and the emergence of an abundant population of mesoscale and sub-mesoscale coherent vortices, no doubt with other phenomena yet to be discovered.

The computational cost varies with horizontal resolution roughly proportional to $1/dx^3$, assuming that the vertical resolution, duration of integration, and domain size are not varied and that $dt \propto dx$ for computational stability and accuracy. This relation implies a thousand-fold disparity in computation costs for any given problem configuration between OGCMs that resolve the eddies and those that do not. Computer limitations, therefore, cause OGCM usage to be split between these two types of configurations. At present, eddy-resolving models can be used well for intervals as long as decades and domains as large as basins, although global calculations are being attempted. In contrast, coarse-resolution models are also suitable for centennial and millennial fluctuations and for approaching equilibrium in global domains. Although growing computer power will narrow this division, it will be at least a decade, and perhaps much longer, before it disappears and everyone will prefer an eddy-resolving model. The fact that OGCMs without eddies and with sensible parameterizations can do reasonably well in calculating the large scale thermohaline circulations, heat and water fluxes, and water mass distributions remains somewhat mysterious and thus must be accepted provisionally; however, it suggests that there is something of a dynamical decoupling between these phenomena and the mesoscale eddies, strong currents,

and other small scale phenomena.

4 The Role of the Ocean in Climate System Models

The scientific problems of ocean circulation and climate have a fundamental mutual dependency. Ocean models have an excessive uncertainty in their surface boundary conditions as specified from observations (Sec. 2.2), and the equilibrium climate of the earth strongly depends upon storage and meridional heat transport by the ocean. A more subtle dependency is that fluctuations in either the atmosphere or ocean may elicit a response in the other medium that importantly alters the evolution by feedbacks. ENSO is the best known example of an interannual *coupled mode* of climate variability. However, both the ocean and atmosphere exhibit many other forms of variability than ENSO, and we do not yet know very well how many of these modes are significantly coupled. The paleoclimate record shows many episodes of rapid surface temperature changes of $\mathcal{O}(10)$ K with a probably global extent, most recently during the Alerod–Younger Dryas fluctuations at the end of the last ice age about 12,000 years ago (Dansgaard et al., 1984). Within the modern era ocean surface temperatures show substantial decadal variability in the regional spatial patterns of atmospheric "teleconnection" modes such as the North Atlantic Oscillation (Deser and M., 1993). My view is that both of these phenomena are related to the delicacy and intrinsic variability of the oceanic thermohaline circulation (Chap. 6). In addition, a new coupled mode is being excited by the radiative forcing from anthropogenic greenhouse gas emissions, which may further involve the thermohaline circulation because of the associated changes in planetary-scale buoyancy forcing.

A coupled climate model includes a global OGCM, together with models for sea ice, the land surface, and the atmosphere. This type of model has a long history of usage (Manabe and Bryan, 1969). It has been the principal means for forecasting global warming due to increasing greenhouse gases, and therefore it will undoubtedly become an even more important tool as mankind begins to practice planetary environmental management. One of the least convincing aspects of coupled models has been the prevalent tendency for *climate drift* away from the actual climate. To avoid this the common practice has been to impose surface *flux corrections* or *flux adjustments* as an artificial stabilization technique. This consists of computing equilibrium states for the uncoupled oceanic and atmospheric models (*e.g.,* using surface (S, T) restoring terms and specified sea surface T, respectively), computing the associated heat and water air-sea fluxes for each model, and then imposing the difference between the models' fluxes as spatially and seasonally varying added source terms to one of the models, usually the ocean. This reduces climate drift in the subsequent coupled solution, and different modeling groups have found differing degrees of drift suppression by this technique.

An obvious goal for coupled modeling is to eliminate flux corrections while avoiding excessive climate drift. Some notable advances towards this goal have occurred, and one example is the recent solution for the NSF/NCAR Climate System Model. Without flux corrections (other than a global air-sea water balance constraint to compensate for the neglect of river inflow to the ocean),

the average air temperature shows no significant drift over an integration of 300 years (Fig. 18; Boville and Gent (1998)). The reasons behind this success appear primarily to be advances in SGS parameterization (clouds and radiation in the atmospheric model, the surface PBL in both models, and isopycnal tracer transport in the ocean model), as well as having an initial condition with an equilibrium, uncoupled ocean solution forced by reasonably accurate surface fluxes. This apparent lack of drift in surface temperature would not continue indefinitely in this calculation, however, since there is appreciable drift in, for example, the oceanic S field associated with the lack of river inflow and excessive water throughput in the sea-ice model, and eventually this would contaminate the surface T. Furthermore, as always, there are many properties of this coupled solution that are unrealistic and warrant further attention.

Achieving skillful coupled models is an important and difficult scientific challenge. There are so many physical processes that must be included for a physically consistent calculation of climate, and probably there are many failure modes that lead to excessive drift. Of course, some blemishes in the simulated oceanic behavior will occur because of failures in the other component models in a coupled solution. Two examples of known problems of this type are an incorrect location of the sea-ice boundary and an excessive amount of surface solar radiation due to underestimation of stratus cloud amounts or cloud absorption in the atmospheric model.

OGCMs must avoid their own contributions to coupled failure modes. The use of surface restoring terms for T and S in ocean models precludes many of these failure modes. To make progress, then, ocean models must evolve away from using this procedure for the buoyancy forcing. This poses a new requirement that an OGCM yield a correct surface T (necessary for correct air-sea fluxes) as a result of the forcing it receives and its own intrinsic variability. In principle, meeting this requirement involves all aspects of the OGCM, but there is probably particular importance to the surface PBL, marginal seas and river inflows, and interactions with sea ice.

For the reasons discussed in Sec. 3.3, OGCMs with coarse spatial grids will be most commonly used in coupled calculations, although some exploratory calculations with eddy-resolving models no doubt will be made. However, the prospect of either not resolving eddies or doing so inaccurately is unpalatable. This gives us added incentive to develop more robust methods for accelerating OGCM solutions (Sec. 2.3) and more skillful parameterizations for marginally resolved eddying solutions, like those used in Large Eddy Simulations (LES) for small-scale turbulence.

5 Summary and Prospects

Models of the oceanic general circulation are currently in a phase of rapid development and expanding utilization. Within the range of legitimate choices for model formulation and boundary conditions, surveyed above, present model solutions do seem to encompass the major features of the observed circulation. In the coming decades the primary challenges are to extend and refine the modeling choices and to expand the observational system to reduce the empirical uncertainties for

testing the models. The goal, of course, is achieve a useful degree of consistency between OGCM solution behaviors and nature (*e.g.,* Fig. 19). The biggest surprises along the way are likely to come from weaning the ocean model from specified, or at least strongly constrained, surface boundary conditions, as it assumes its proper, more fundamental role in modeling Earth's climate system.

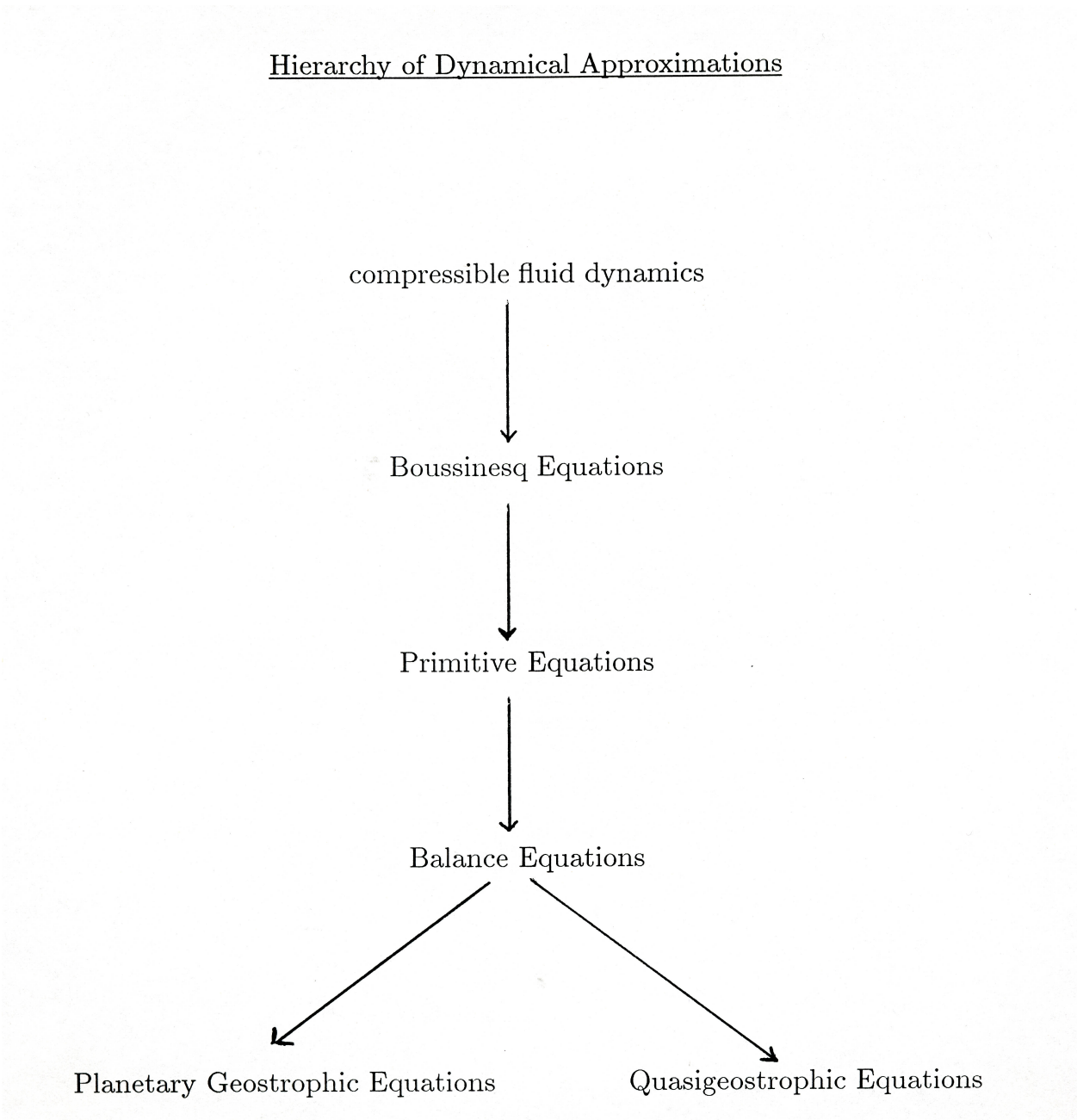

Figure 1: A hierarchy of dynamical approximations.

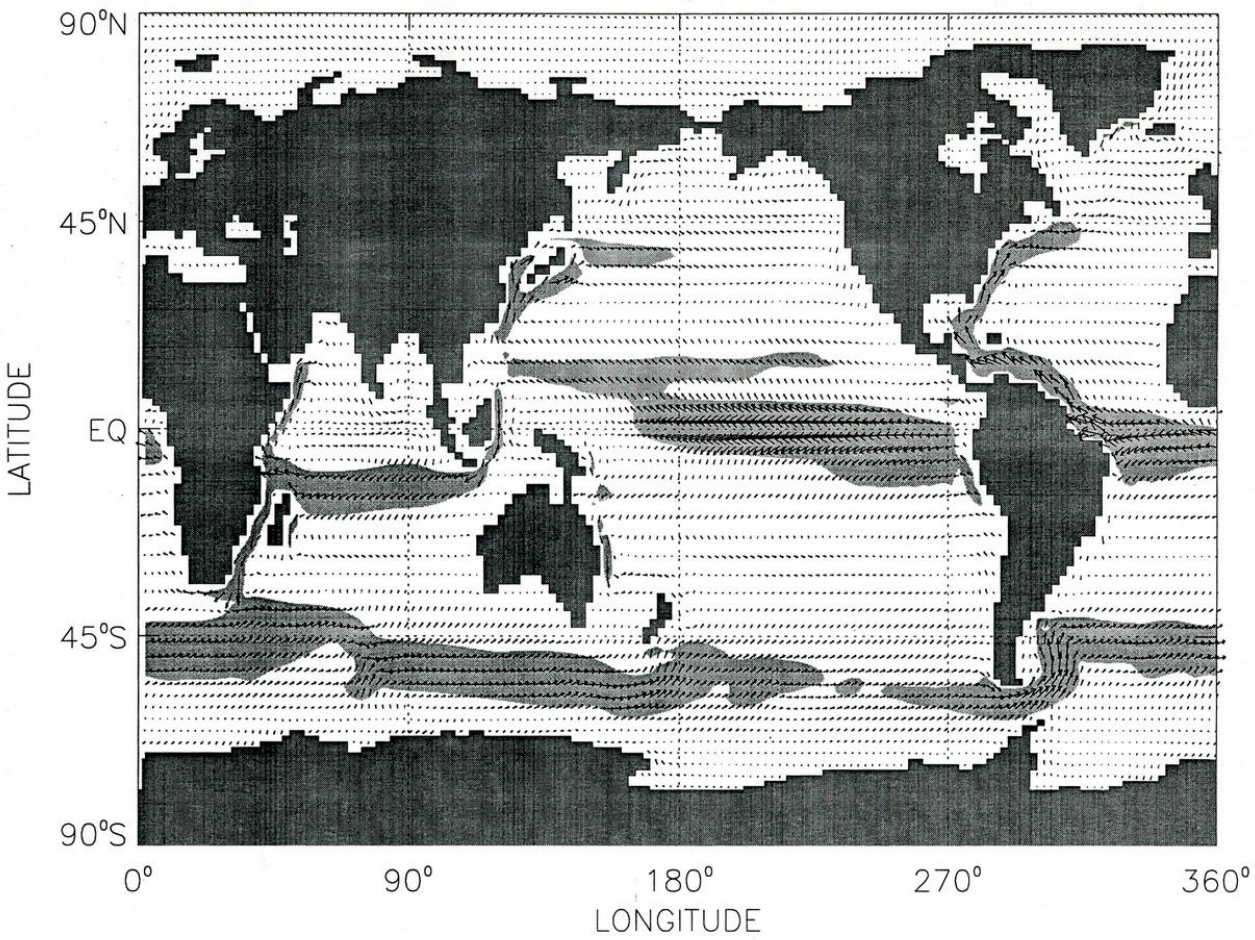

Figure 2: Time-mean surface currents from a coarse-resolution OGCM. Speeds greater than 0.1 m s^{-1} are shaded, and the maximum vector length is 0.55 m s^{-1} (Gent et al., 1998).

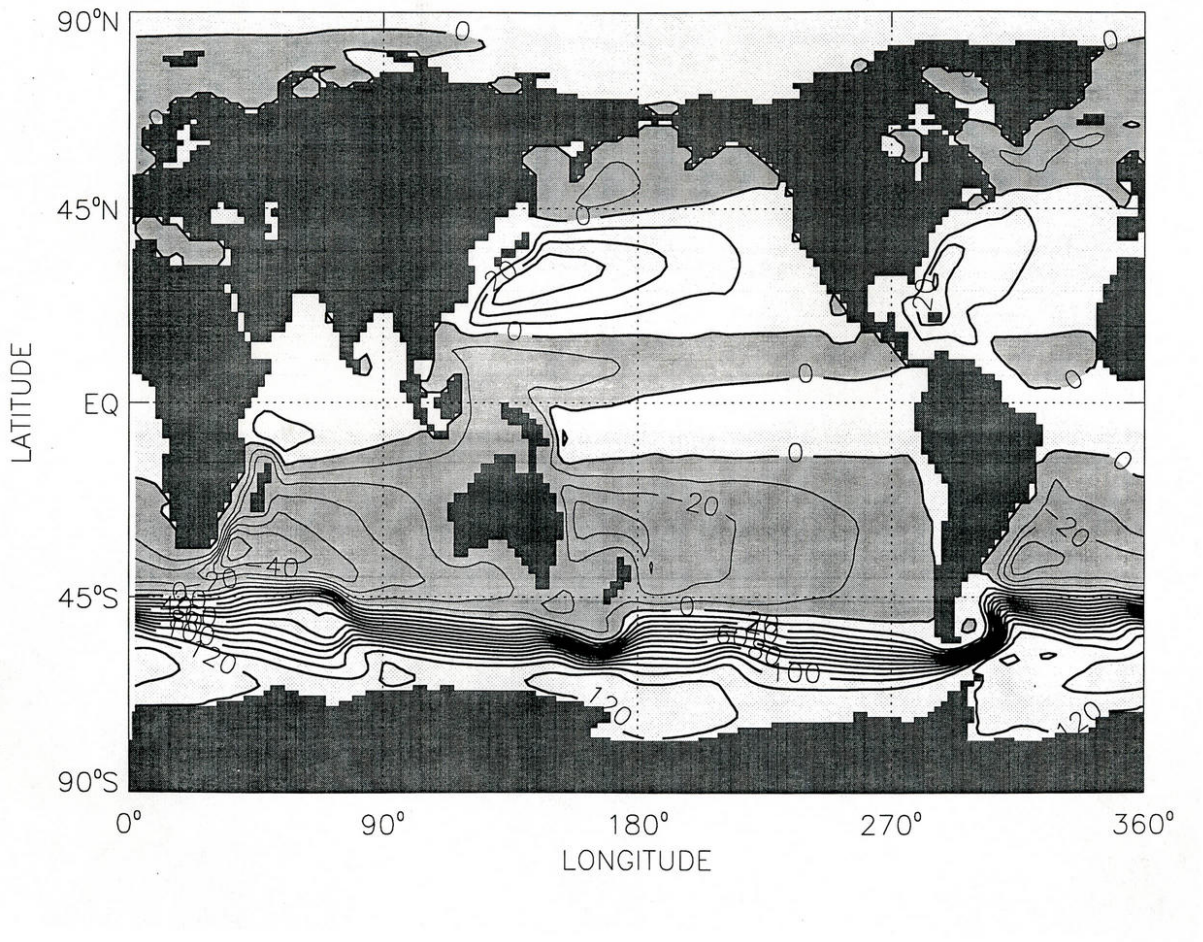

Figure 3: Time-mean barotropic streamfunction from a coarse-resolution OGCM. Counterclockwise circulation is shaded. The contour interval is 10 Sv (1 Sv $= 10^6$ m^3 s^{-1}) (Gent et al., 1998).

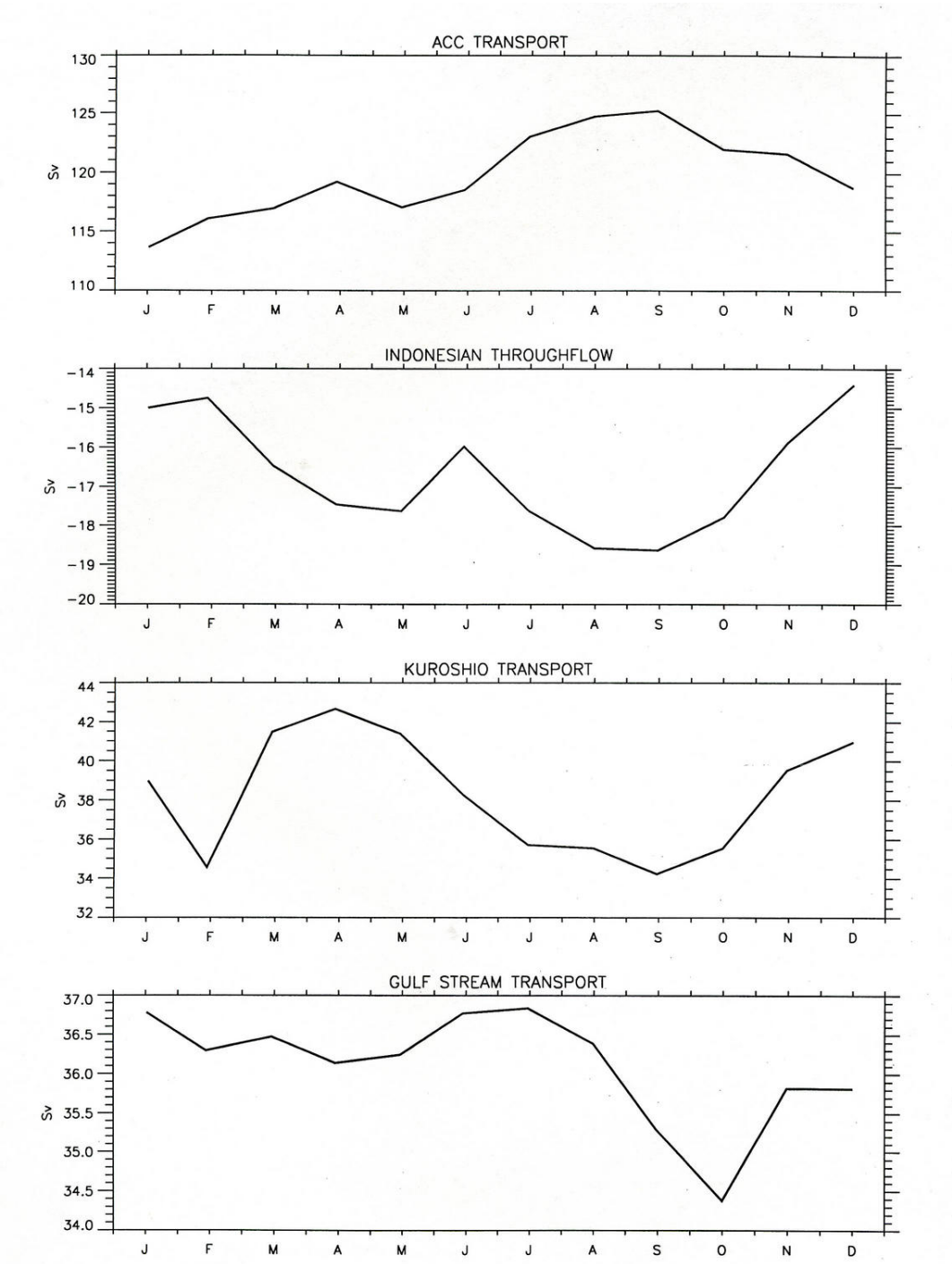

Figure 4: Annual cycle of horizontal transport across selected currents from a coarse-resolution OGCM: (a) Antarctic Circumpolar Current (Drake Passage); (b) Indonesian Throughflow; (c) Kuroshio (26^o N); (d) Gulf Stream (29^o N) (Gent et al., 1998).

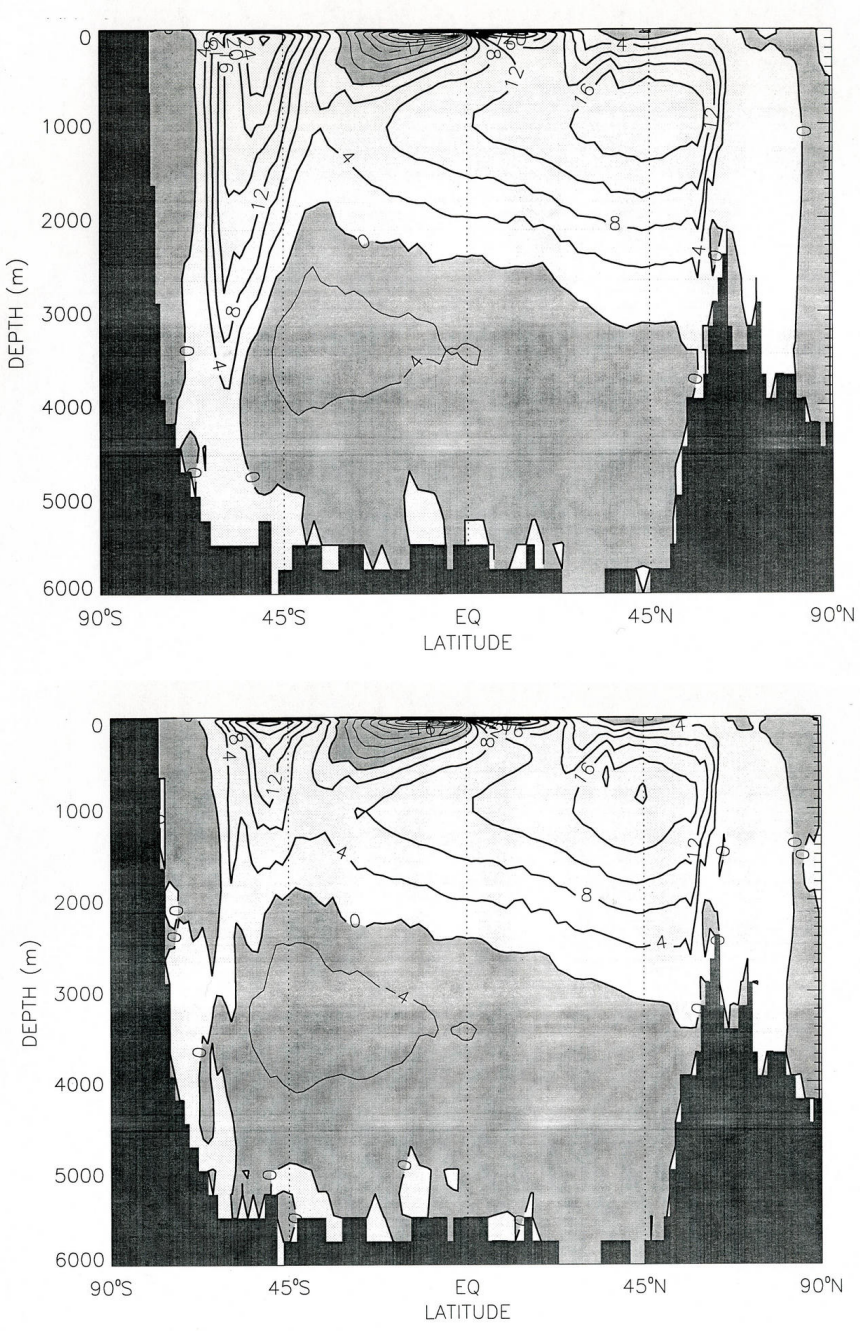

Figure 5: Time-mean meridional transport streamfunction from a coarse-resolution OGCM: (top) Eulerian flow; (bottom) total Lagrangian flow including the eddy-induced transport velocity. Counterclockwise circulation is shaded. The contour interval is 4 Sv (Gent et al., 1998).

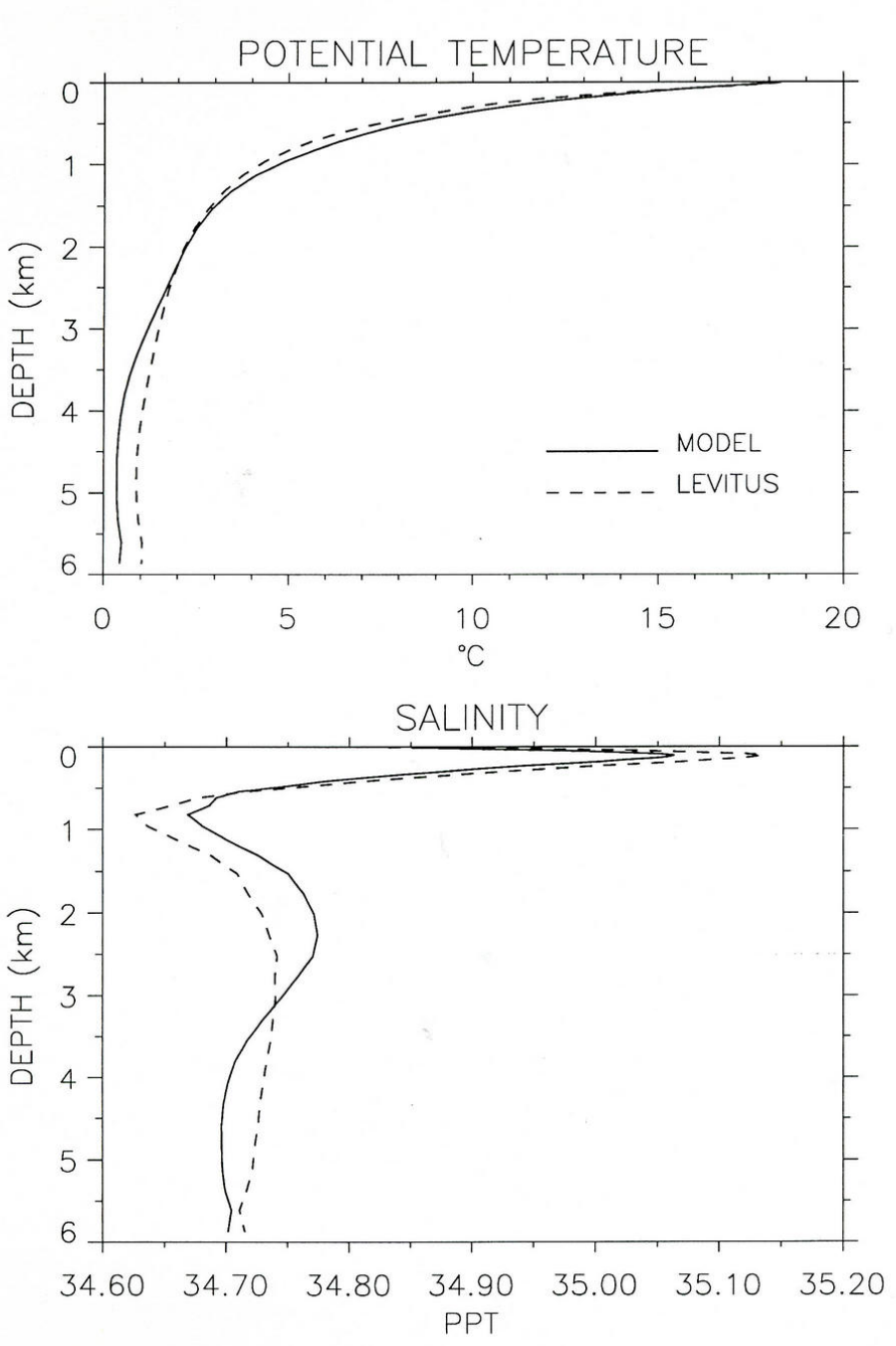

Figure 6: Time- and horizontal-mean profiles of T and S from a coarse-resolution OGCM and from Levitus (1982) (Gent et al., 1998).

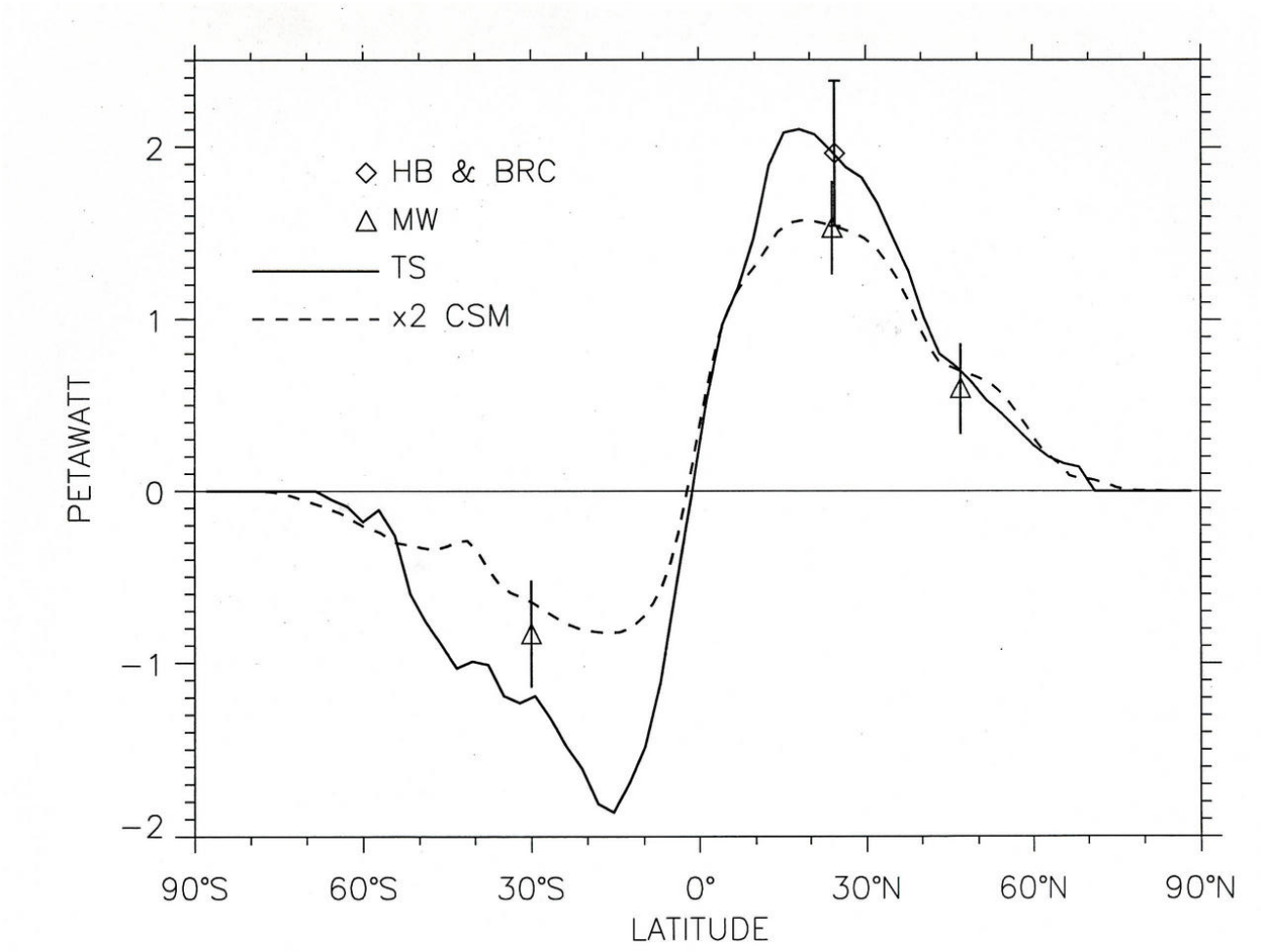

Figure 7: Time-mean northward heat transport from a coarse-resolution OGCM (Gent et al., 1998) and from empirical estimates (and their uncertainty) by Hall and Bryden (1982), Bryden et al. (1991), Trenberth and Solomon (1994), and MacDonald and Wunsch (1996).

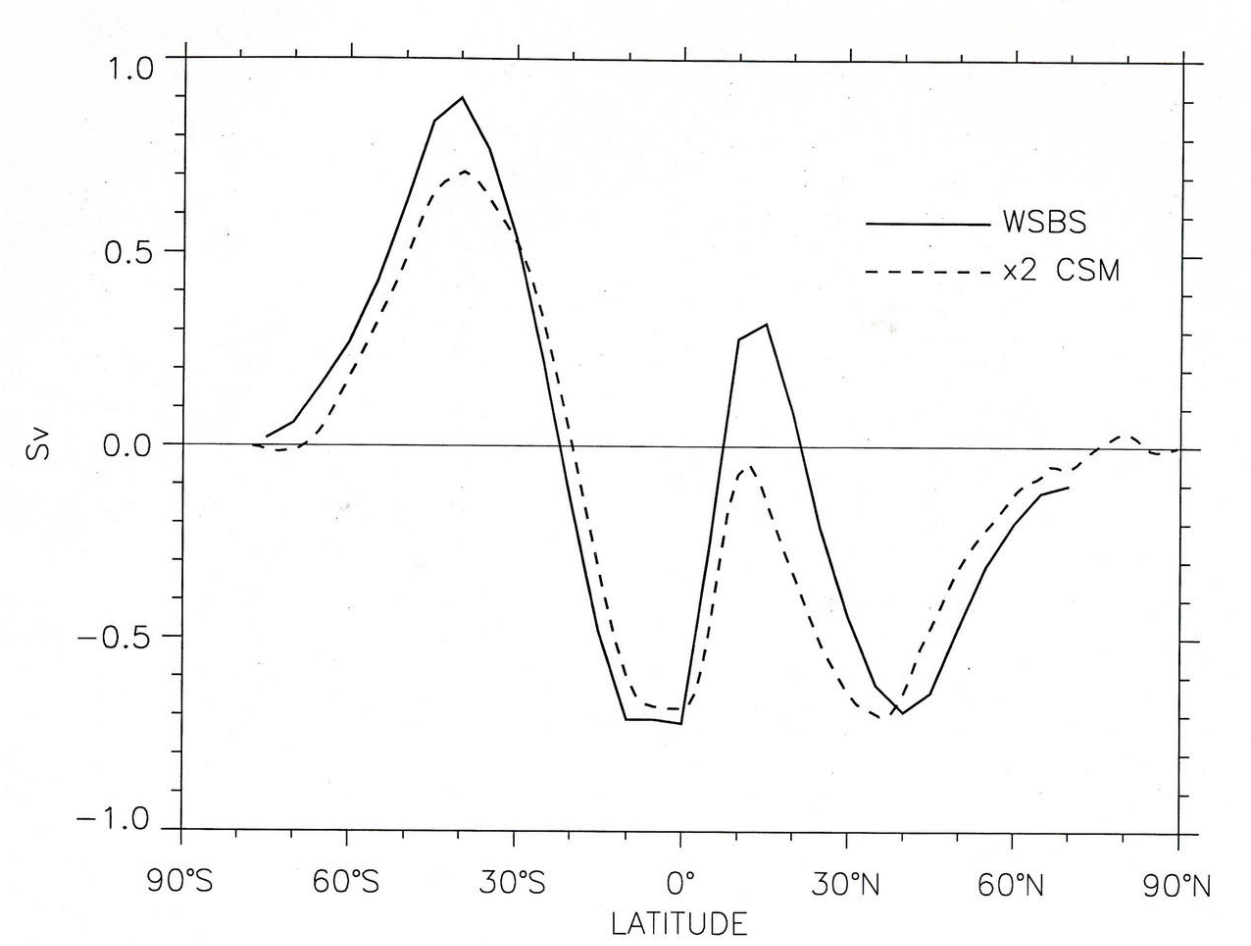

Figure 8: Time-mean northward water transport from a coarse-resolution OGCM (Gent et al., 1998) and from empirical estimates by Wijffels et al. (1992).

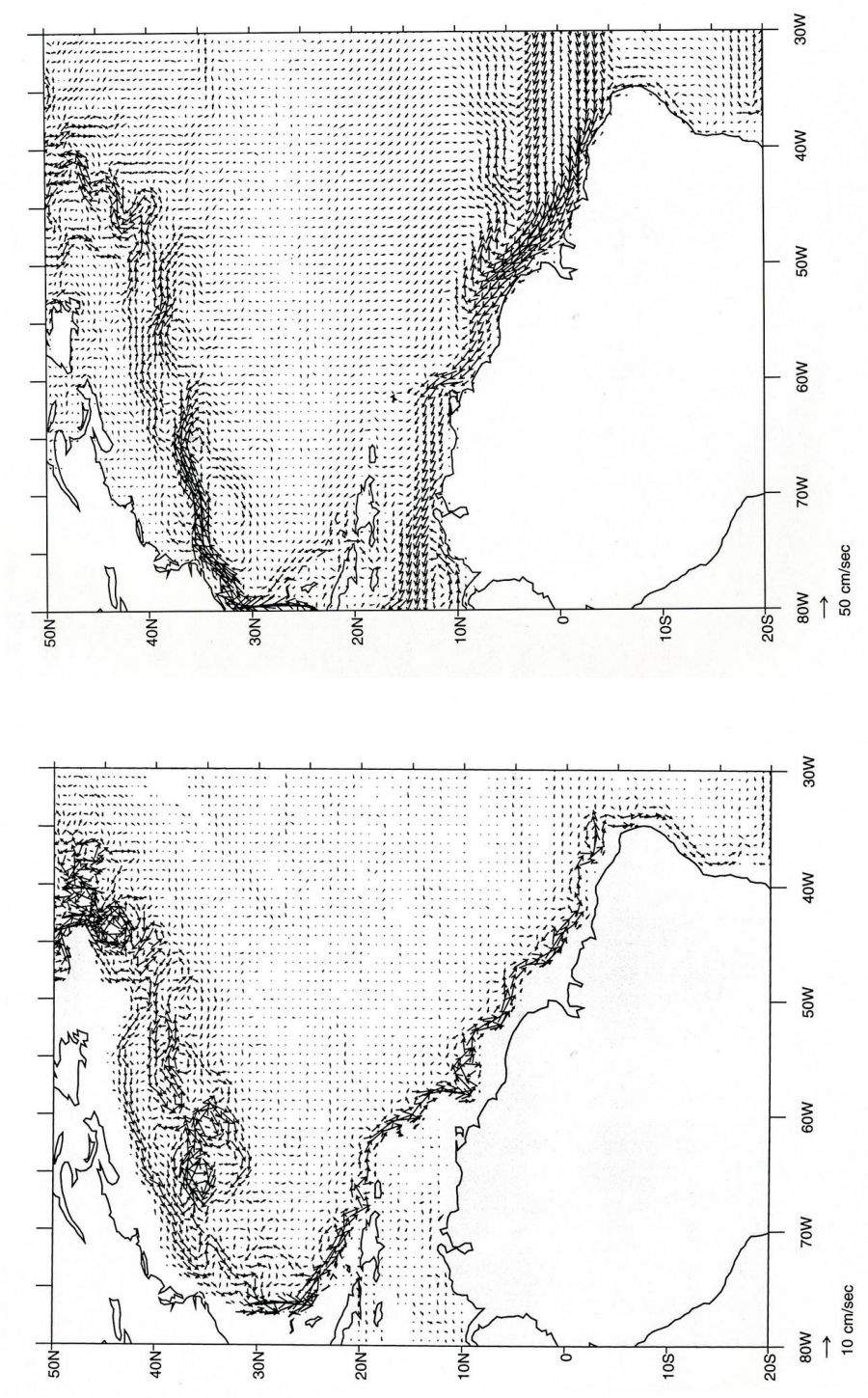

Figure 9: Time-mean currents from a fine-resolution OGCM for the Atlantic basin: (top/right) 15 m depth and (bottom/lrgy) 2500 m depth (Smith et al., 2000). Only a portion of the domain is plotted here.

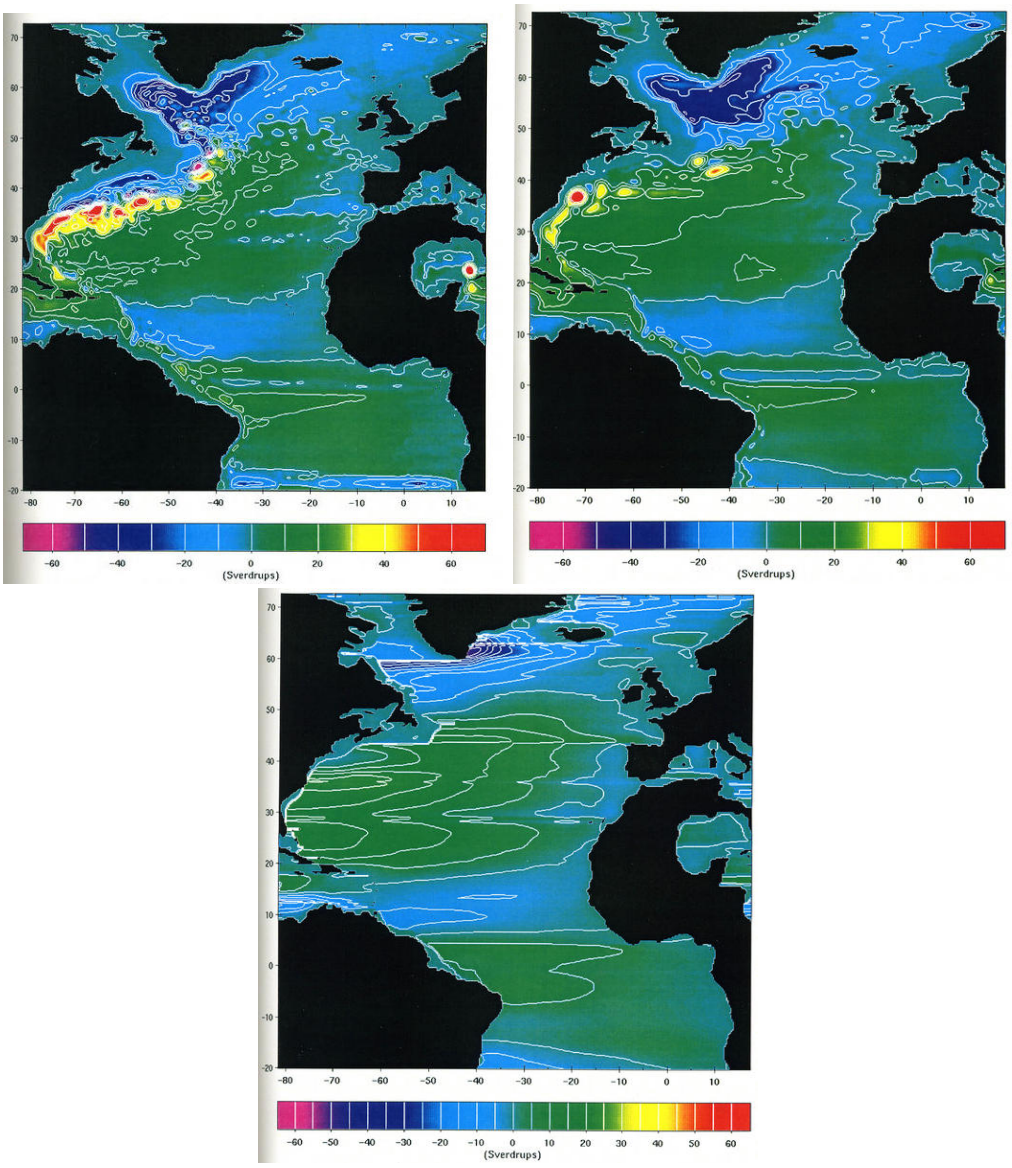

Figure 10: Mean barotropic streamfunction in an eddy-resolving OGCM for the North Atlantic ocean: (top left) $\Delta\phi = 0.1^o$; (top right) $\Delta\phi = 0.25^o$. The bottom plot is the Sverdrup transport for the same wind stress (Smith et al., 2000).

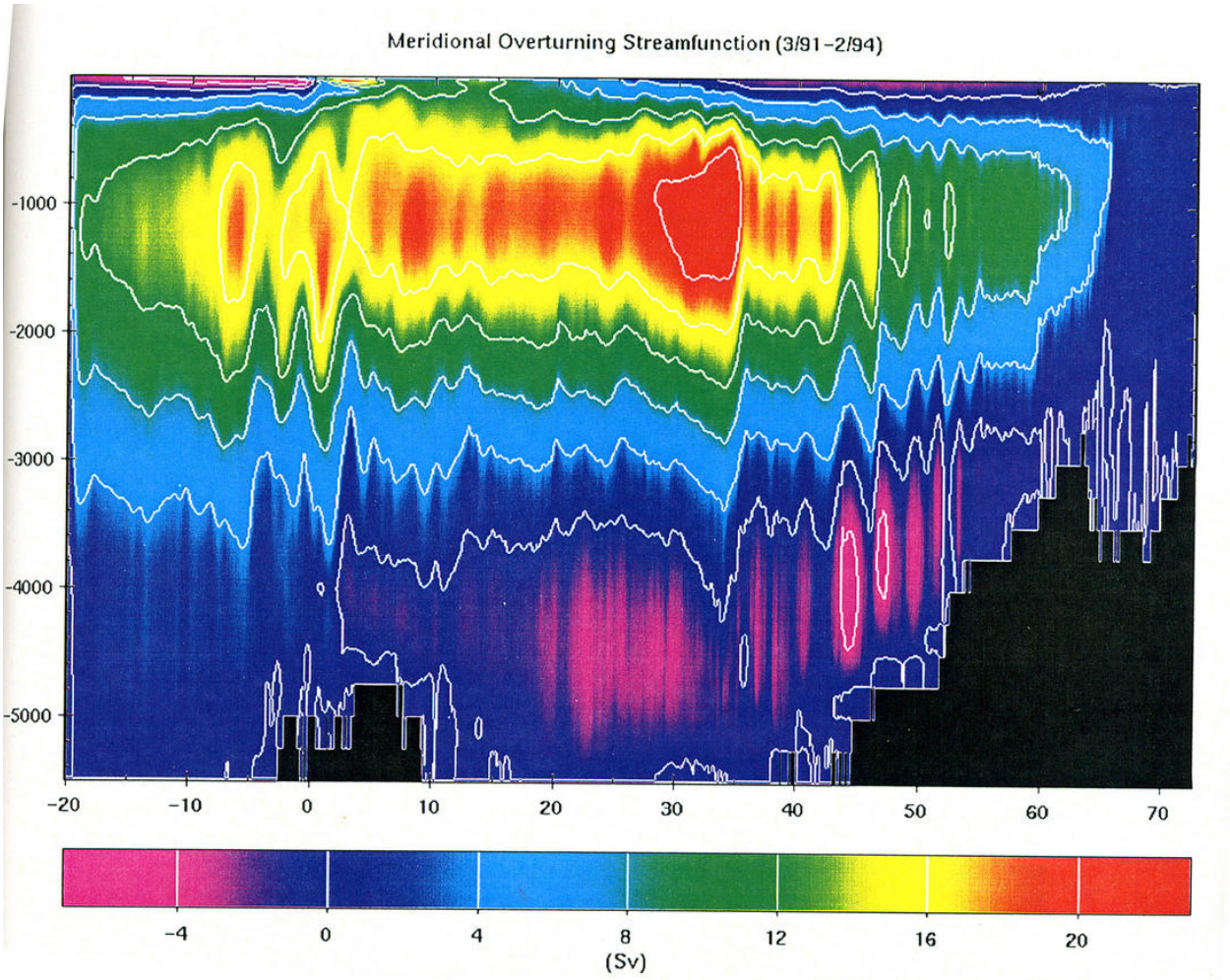

Figure 11: Mean meridional overturning circulation in an eddy-resolving OGCM for the North Atlantic ocean with $\Delta\phi = 0.1^o$ (Smith et al., 2000).

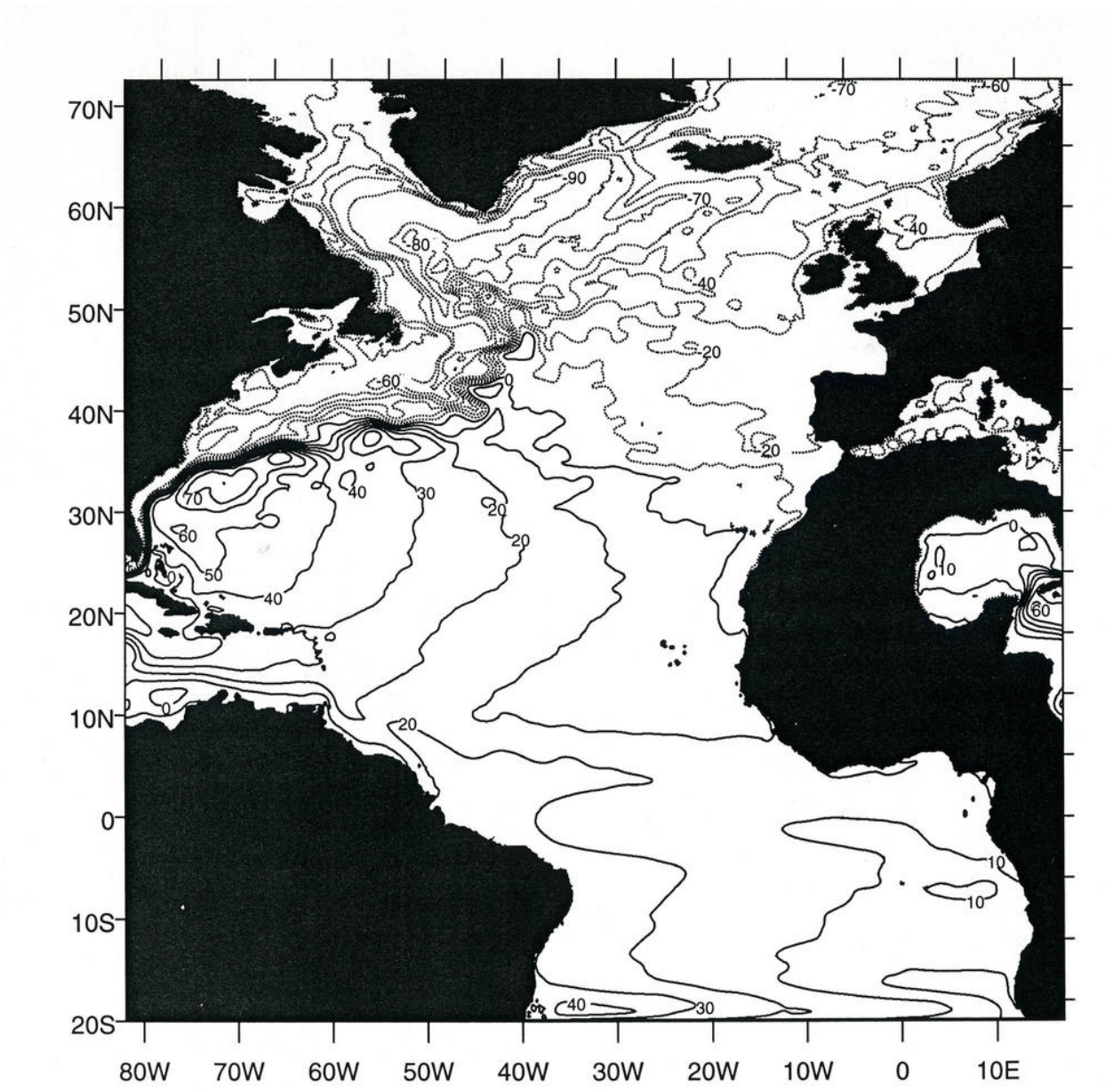

Figure 12: Time-mean sea surface elevation from a fine-resolution OGCM for the Atlantic basin. The contour interval is 10 cm (Smith et al., 2000).

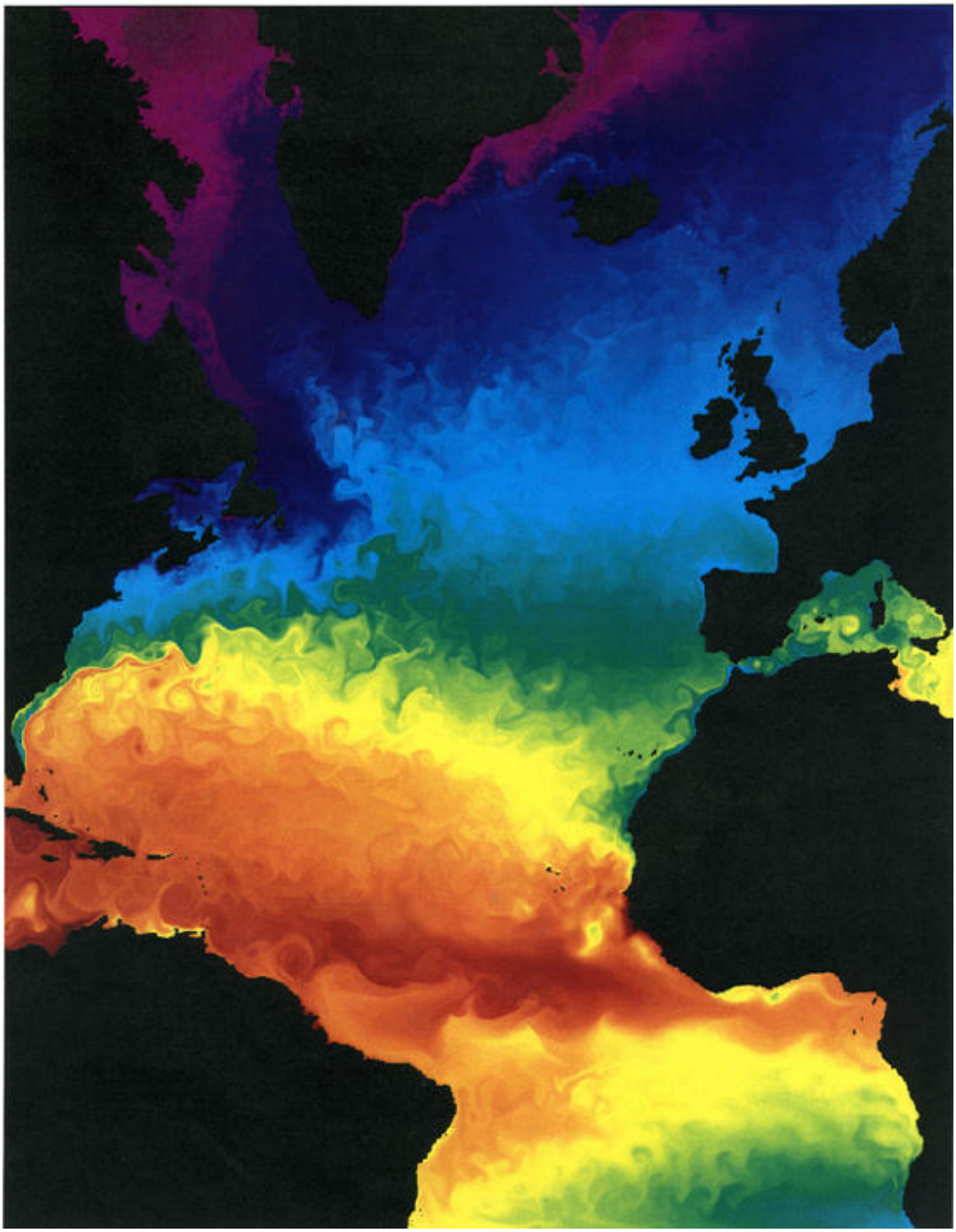

Figure 13: Instantaneous sea surface temperature from a fine-resolution OGCM for the Atlantic basin (Smith et al., 2000).

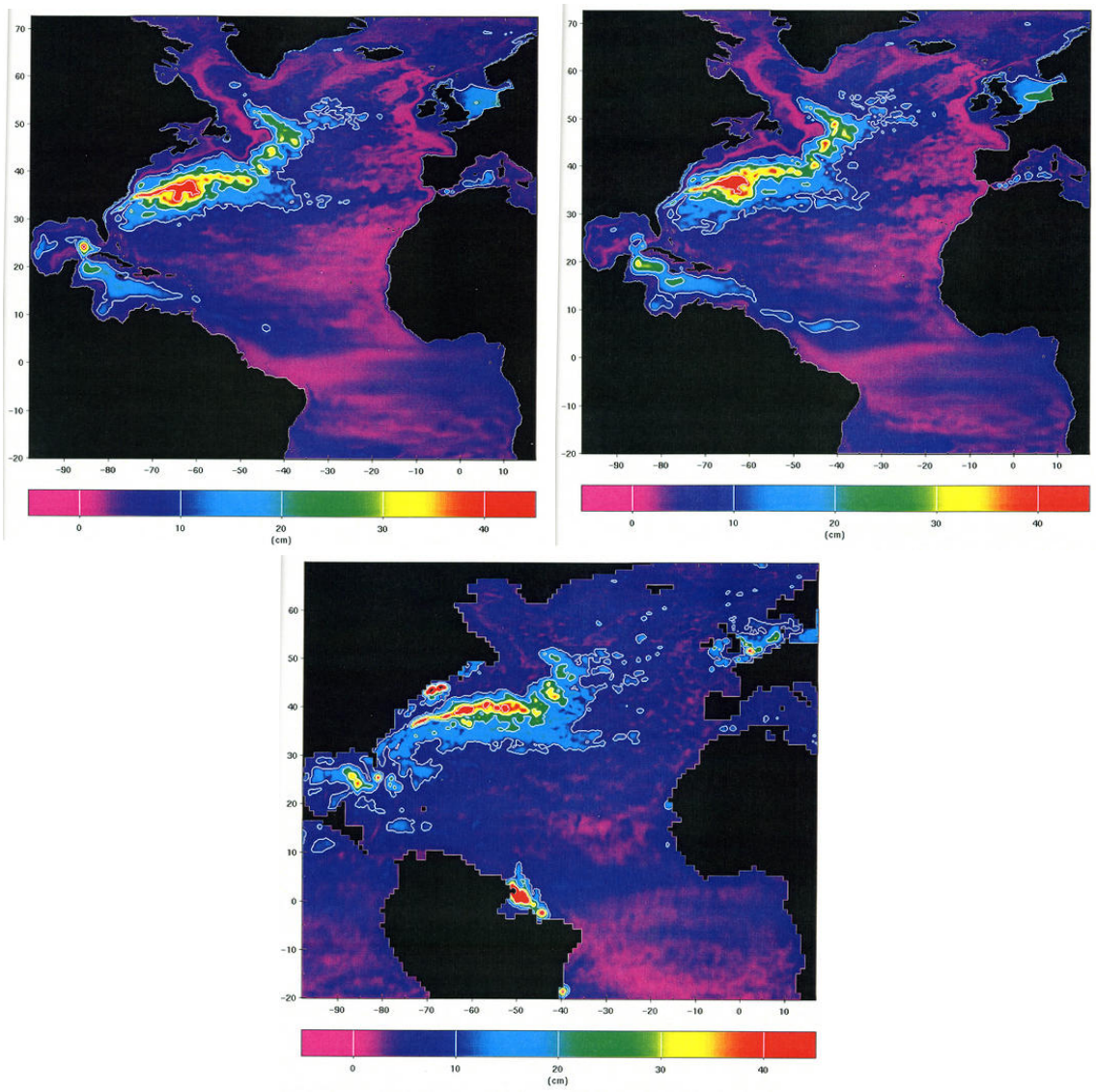

Figure 14: R.m.s. sea level variability in an eddy-resolving OGCM for the North Atlantic Ocean: (top left) 1984-1989; (top right) 1991-1994. The bottom plot is the observed variability for the latter period (Smith et al., 2000).

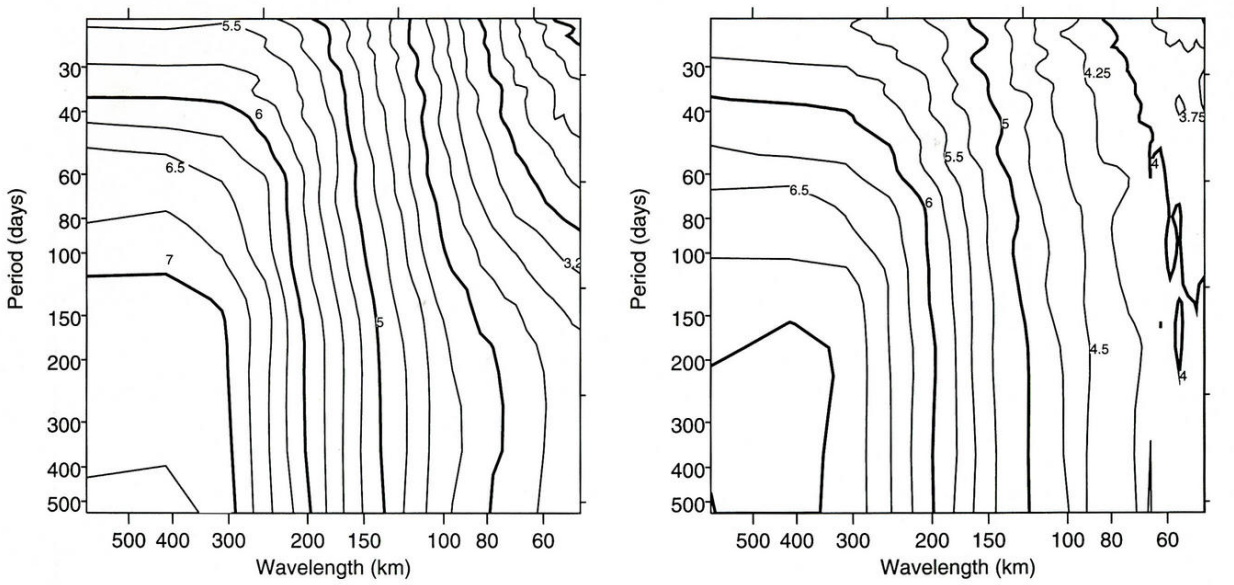

Figure 15: Wavenumber-frequency spectra of sea-surface elevation in the Gulf Stream region, 50-75^o W, 32-42^o N: (left) from a fine-resolution OGCM for the Atlantic basin; (right) from TOPEX/Poseidon altimeter measurements (Smith et al., 2000).

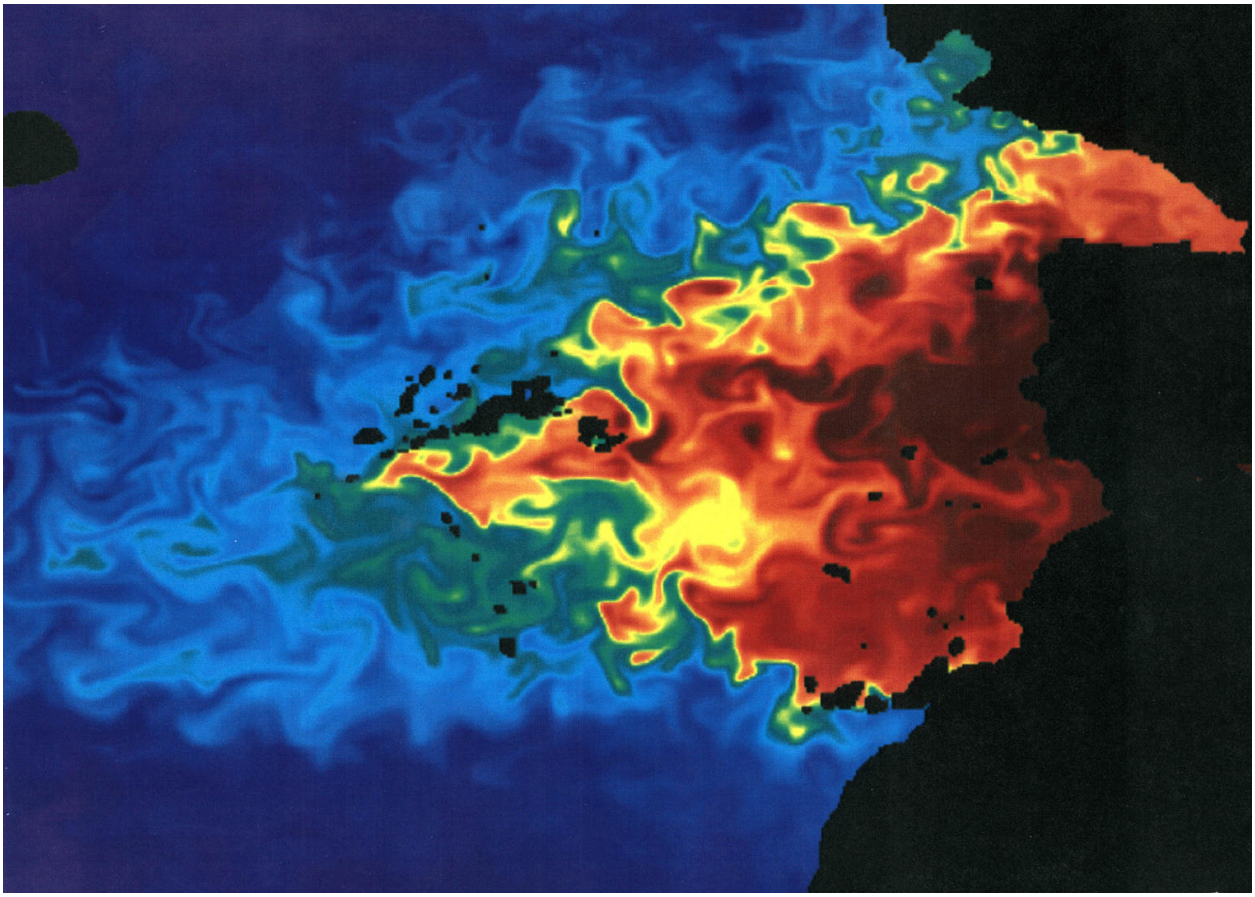

Figure 16: Salinity near the Mediterranean at a depth of 1140 m from a fine-resolution OGCM for the Atlantic basin. Red represents the warm-salty water from the Mediterranean outflow and blue the cold-fresh water of the interior Atlantic Ocean (Smith et al., 2000).

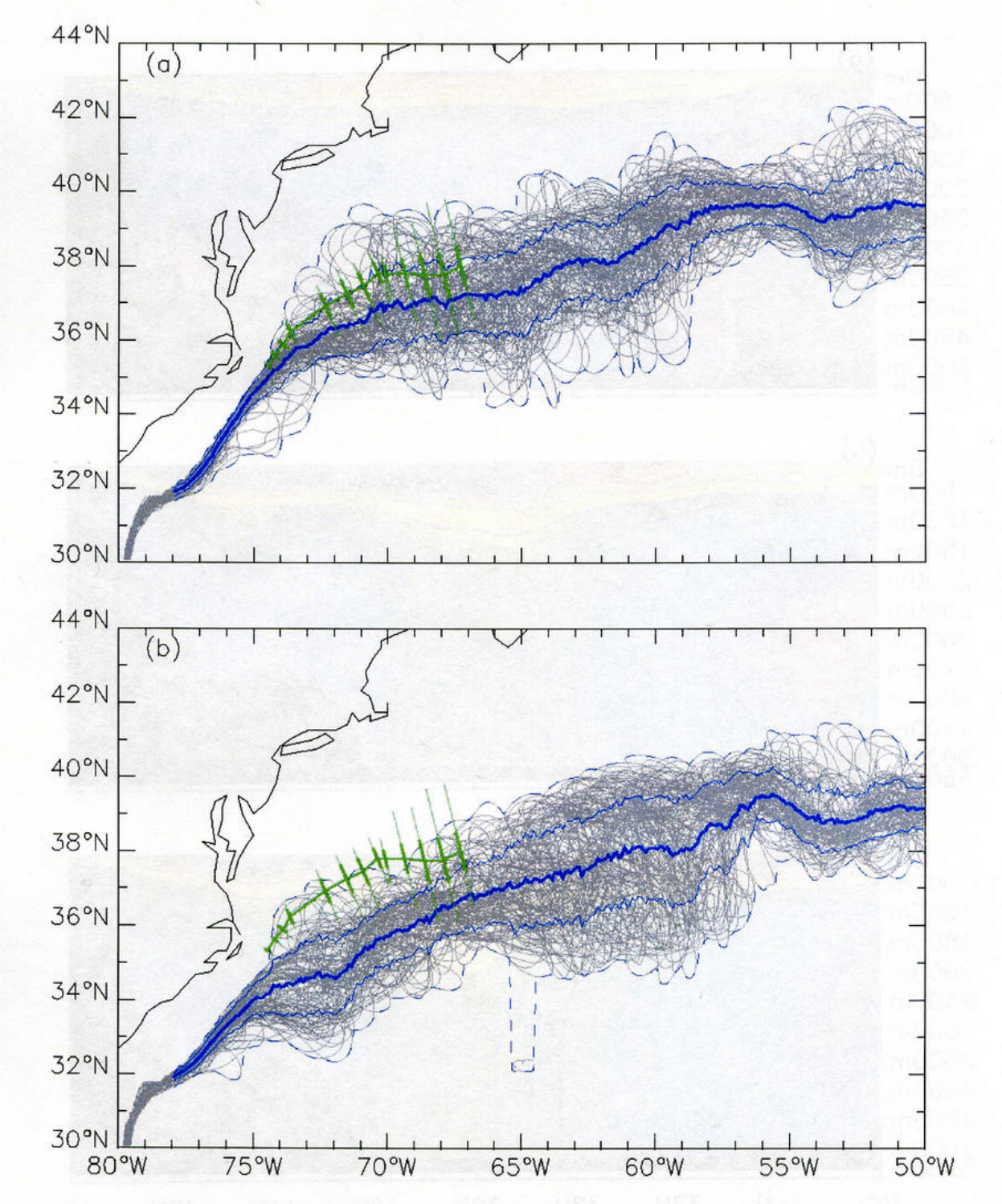

Figure 17: Gulf stream path defined by the 12 C isotherm at 400 m every 10 days during 1998-2000 for two eddy-resolving OGCMs. The mean position and one standard deviation envelope are indicated by solid blue curves, and the observed position and variability are indicated in green (Bryan et al., 2006).

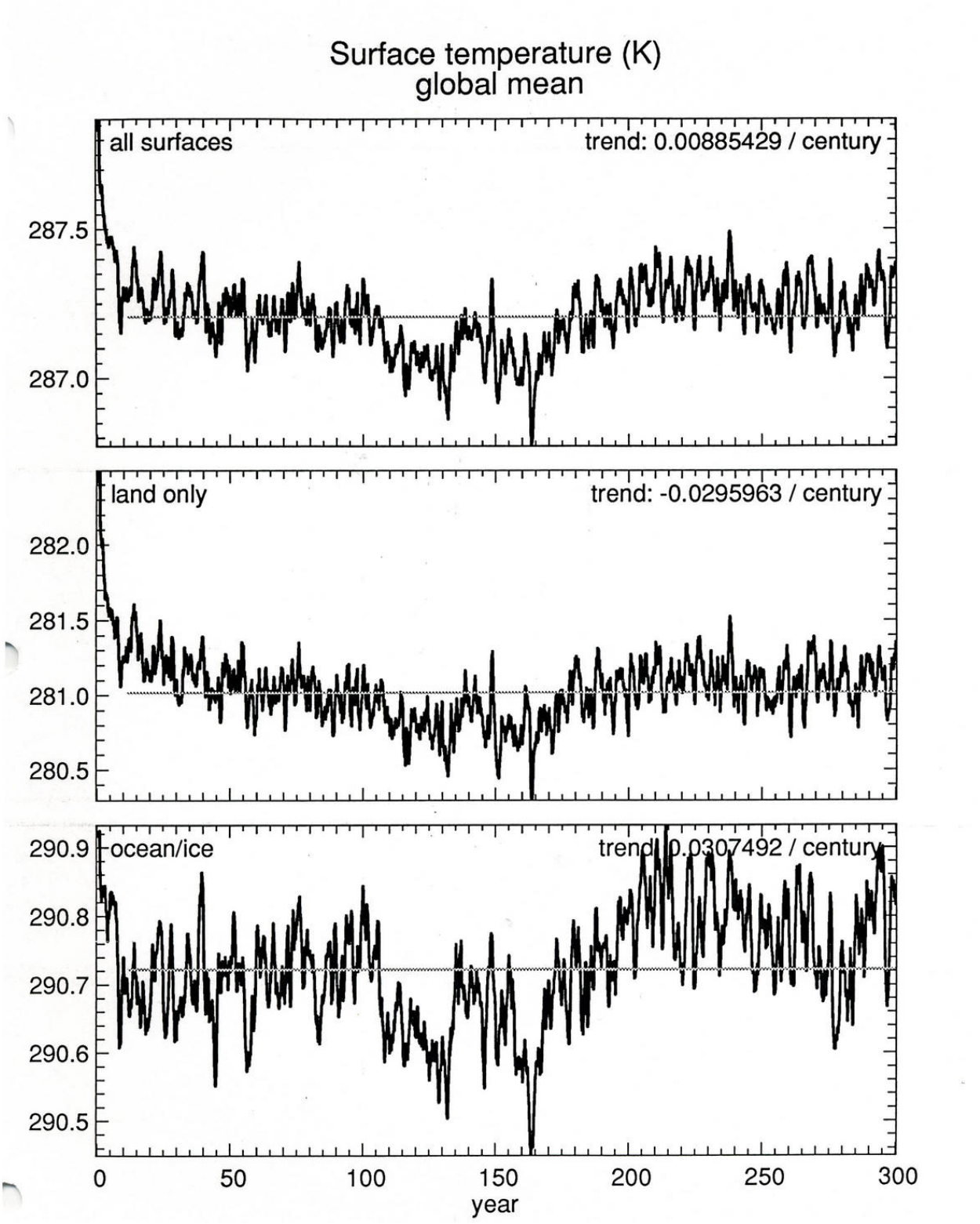

Figure 18: Time series of spatially averaged surface air temperature in a 300-year integration of the NCAR Climate System Model (Boville and Gent, 1998).

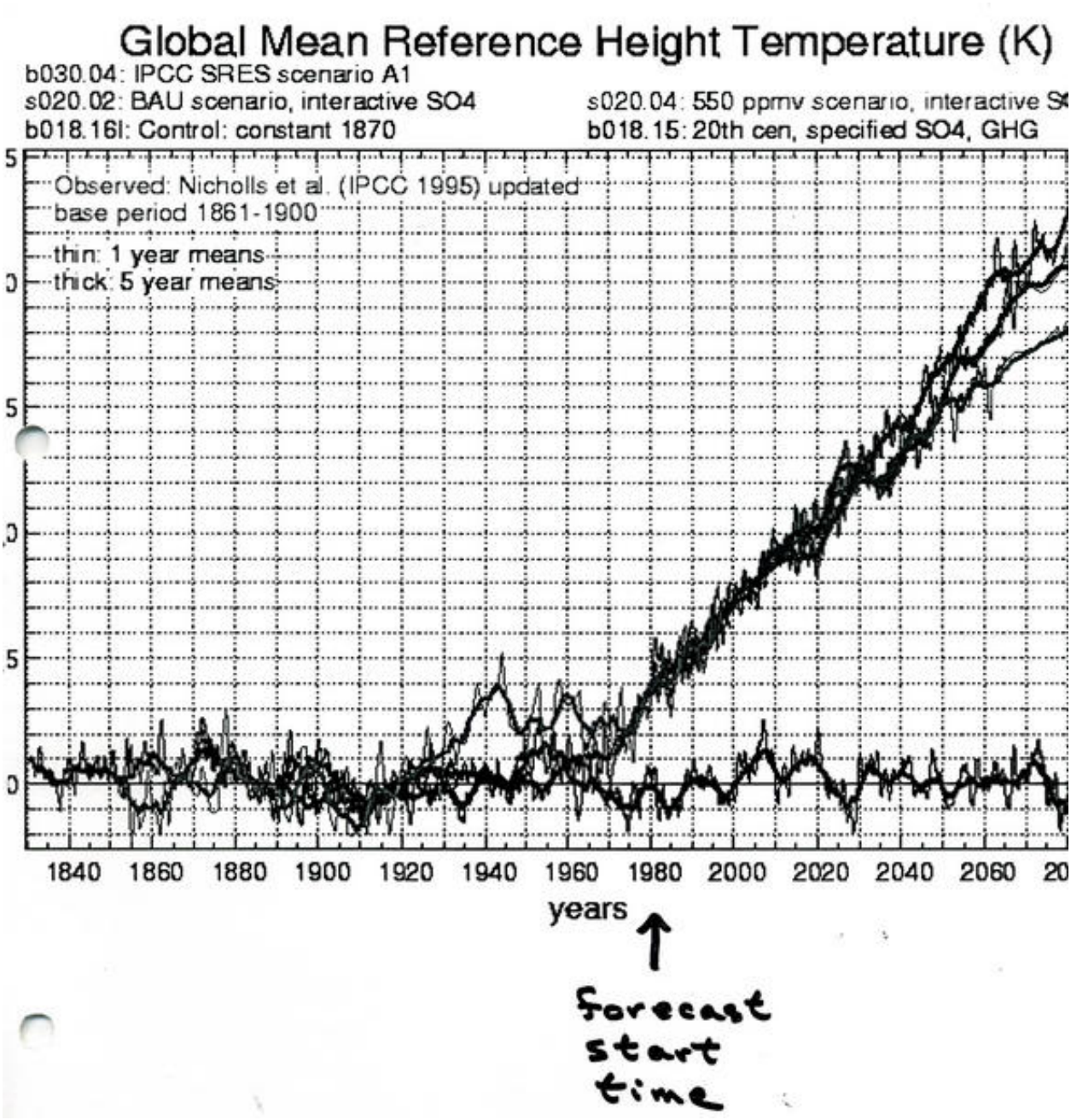

Figure 19: Time series of spatially averaged surface air temperature in a several integrations of the NCAR Climate System Model for the past period with reconstructed emission histories and for the next century with hypothetical emisions (Dai et al., 2001). The ordinate range is from 0 to 2.5 C.

References

Barnier, B., L. Siefridt, and P. Marchesiello: 1995, Thermal forcing for a global ocean circulation model using a three-year climatology of ECMWF analyses. *J. Marine Sys.*, **6**, 363–380.

Beckmann, A. and R. Döscher: 1997, A method for improved representation of dense water spreading over topography in geopotential-coordinate models. *J. Phys. Ocean.*, **27**, 581–591.

Boville, B. and P. Gent: 1998, Century integrations with the NCAR Climate System Model. *J. Clim.*, **11**, 1115–1130.

Bryan, F., M. Hecht, and R. Smith: 2006, Resolution convergence and sen sitivity studies with North Atlantic circulation models. Part 1: The western boundary current system. *Ocean Modelling*, submitted.

Bryan, K.: 1969, A numerical method for the study of the circulation of the world ocean. *Comp. Phys.*, **4**, 347–376.

Bryden, H., D. Roemmich, and J. Church: 1991, Ocean heat transport across 24 n in the Pacific. *Deep Sea Res.*, **38**, 297–324.

Covey, C.: 1995, Global ocean circulation and equator-pole heat transport as a function of ocean GCM resolution. *J. Clim.*, **11**, 425–437.

Dai, A., T. Wigley, B. Boville, J. Kiehl, and L. Buja: 2001, Climates of the 20th and 21st centuries simulated by the NCAR Climate Systems Model. *J. Clim.*, **14**, 485–519.

Dansgaard, W., S. Johnson, H. Clausen, D. Dahl-Jensen, N. Gundestrup, C. Hammer, and H. Oeschger: 1984, North atlantic climatic oscillations revealed by deep Greenland ice cores. *Climate Processes and Climate Sensitivity*, J. Hansen and T. Takahashi, eds., A.G.U., 288–298.

Deser, C. and B. M.: 1993, Surface climate variations over the North Atlantic Ocean during winter: 1900-1989. *J. Clim.*, **6**, 1743–1753.

Ferrari, R. and J. McWilliams: 2006, Parameterization of eddy fluxes near oceanic boundaries. *J. Clim.*, submitted.

Gent, P., F. Bryan, G. Danabasoglu, S. Doney, W. Holland, W. Large, and J. McWilliams: 1998, The NCAR Climate System Model global ocean component. *J. Clim.*, **11**, 1287–1306.

Gent, P. and J. McWilliams: 1990, Isopycnal mixing in ocean circulation models. *J. Phys. Ocean.*, **20**, 150–155.

Griffies, S.: 2004, *Fundamentals of Ocean Climate Models*. Princeton University Press, 518 pp.

Hall, M. and H. Bryden: 1982, Direct estimates and mechanisms of ocean heat transport. *Deep Sea Res.*, **29**, 339–359.

Large, G., W. Danabasoglu, S. Doney, and J. McWilliams: 1997, Sensitivity to surface forcing and boundary layer mixing in a global ocean model: Annual-mean climatology. *J. Phys. Ocean.*, **27**, 2418–2447.

Large, G., W. Danabasoglu, J. McWilliams, P. Gent, and F. Bryan: 2001, Equatorial circulation of a global ocean climate model with anisotropic horizontal viscosity. *J. Phys. Ocean.*, **31**, 518–536.

Large, W., J. McWilliams, and S. Doney: 1994, Oceanic vertical mixing: A review and a model with a non-local K-profile boundary layer parameterization. *Rev. Geophys.*, **32**, 363–403.

Levitus, S.: 1982, *Climatological Atlas of the World Ocean*. NOAA Prof. Paper 13, 173 pp.

MacDonald, A. and C. Wunsch: 1996, An estimate of global ocean circulation and heat fluxes. *Nature*, **382**, 436–439.

Manabe, S. and K. Bryan: 1969, Climate calculations with a combined ocean-atmosphere model. *J. Atmos. Sci.*, **26**, 786–789.

Marchesiello, P., J. McWilliams, and A. Shchepetkin: 2001, Open boundary conditions for long-term integration of regional ocean models. *Ocean Modelling*, **3**, 1–20.

McWilliams, J.: 1998, Oceanic general circulation models. *Ocean Modeling and Parameterization*, E. C. . J. Verron, ed., Kluwer, 1–44.

Shchepetkin, A. and J. McWilliams: 2005, The regional oceanic modeling system (ROMS): A split-explicit, free-surface, topography-following-coordinate oceanic model. *Ocean Modelling*, **9**, 347–404.

— 2006, Computational kernel algorithms for fine-scale, multi-process, long-term oceanic simulations. *Handbook of Numerical Analysis: Computational Methods for the Ocean and the Atmosphere*, T. R. and J. Tribbia, eds., Elsevier Science Press, in press.

Smith, R., M. Maltrud, M. Hecht, and F. Bryan: 2000, Numerical simulation of the North Atlantic Ocean at 1/10 degree. *J. Phys. Ocean.*, **30**, 1532–1561.

Smith, R. and J. McWilliams: 2003, Anisotropic horizontal viscosity for ocean models. *Ocean Modelling*, **48**, 129–156.

Trenberth, K. and A. Solomon: 1994, The global heat balance: Heat transports in the atmosphere and ocean. *Clim. Dyn.*, **10**, 107–134.

Wajsowicz, R.: 1993, A consistent formulation of the anisotropic stress tensor for use in models of the large-scale ocean circulation. *J. Comp. Phys.*, **105**, 333–338.

Wijffels, S., R. Schmitt, H. Bryden, and A. Stigebrandt: 1992, Transport of freshwater by the oceans. *J. Phys. Ocean.*, **22**, 155–162.